SSEN Annual Postgraduate Research Symposium 2023

Reid, Rebecca; Samuel, Oluwafemi; Valantinas, Laurynas; Namanqani, Hussam; Marland, Victoria; Mcintosh, Claire

DOI:
10.20933/100001288

Publication date:
2023

Document Version
Publisher's PDF, also known as Version of record


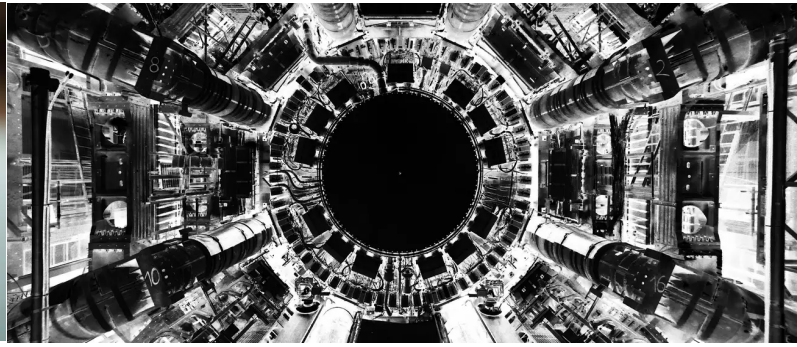

University of Dundee

SCHOOL OF SCIENCE AND ENGINEERING

Annual Postgraduate Research Symposium 2023

11 - 12 May 2023

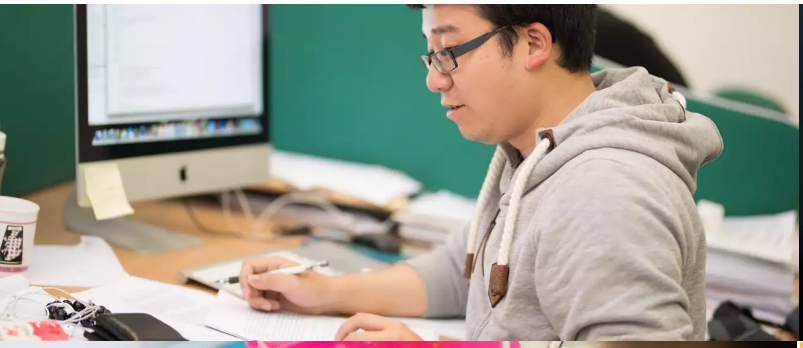


SSEN Postgraduate Research Symposium 2023 – Final Programme

Thursday 11th May 2023

Time	Presenter	Title
0900 – 0930	**Registration and coffee** (Dalhousie Foyer)	
0930 – 0945	**Welcome & Introductions (Blair Grubb, Wendy Alexander, Jose Fiadeiro)**	
0945 – 1030	**Niamh Nic Daéid**	Keynote Lecture: Research with impact – how to communicate your work and make change happen
Session 1	Chair: Thomas Jones + PGR (Dalhousie Lecture Theatre 1)	
1040 – 1100	**Rebecca Reid**	*Developmental changes in the internal architecture of the human distal tibia* ***(CAHID)***
1100 – 1120	**Oluwafemi Samuel**	*Effectiveness of Biometric Technology in the Context of an African Election: Investigating the Possible Causes of Fingerprint Verification Failures* ***(Comp)***
1120 – 1140	**Laurynas Valantinas**	*Diagonally Scanned Airy Light-Sheet* ***(Phys)***
1140 – 1200	**Coffee break** (Dalhousie Foyer)	
Session 2	Chair: Jonathan Knappett + PGR (Dalhousie Lecture Theatre 1)	
1200 – 1220	**Hussam Namanqani**	*A review of lean communication practices for construction mega-projects in Saudi Arabia* ***(Civil)***
1220 – 1240	**Victoria Marland**	*Changing Trends in Benzodiazepine Use Within Scottish Prisons: Detection, Prevalence and Modes of Use* ***(LRCFS)***
1240 – 1310	**Poster presentations 1**	ENG (Biomed, Civil, Mech) – 13 posters
1310 – 1430	**Lunch, poster session and group photograph** (Dalhousie Foyer)	
Session 3	Chair: Dumitru Trucu + PGR (Dalhousie Lecture Theatre 1)	
1430 – 1450	**Claire McIntosh**	*Current Practice in Stature Estimation* ***(CAHID)***
1450 – 1510	**Nader Alharbi**	*The Effectiveness of Blended Learning in Mathematics for Secondary School Students and their Teachers and Parents in Saudi Arabia* ***(Math)***
1510 – 1530	**Poster presentations 2**	CAHID, LRCFS, MATHS, COMP – 10 posters
1530 – 1550	**Coffee break** (Dalhousie Foyer)	
Session 4	Chair: Julieta Gomez-Garcia + PGR (Dalhousie Lecture Theatre 1)	
1550 – 1610	**Maciej Jozwik**	*Fairly and Rapidly Assessing Slowly Reacting Cement Concrete* ***(Civil)***
1610 – 1630	**Yuhang Dong**	*Development and Evaluation of Ag-PTFE-TiO_2 Based Nano-composite Coatings for Preventing Catheter-Associated Infections* ***(Mech)***
1630 – 1650	**Ella Schad**	*The Adventure of Argument: Narrative and Reasoning in Fictionalised Crime* ***(Comp)***
1650	**Concluding remarks (Day 1) (Alan Cuthbertson)**	
1700 – 1800	**Drinks reception and poster session** (Dalhousie Foyer)	

Friday 12th May 2023

Time	Presenter	Title
0930 – 0940	**Welcome Day 2 (Amin Abdolvand)**	
0940 – 1000	**Philippa Sterlina (LLC)**	Open and FAIR Data at University of Dundee - Funder requirements and how to meet them
Session 5	Chair: Lorna Nisbet + PGR (Dalhousie Lecture Theatre 2)	
1000 – 1020	**Steven Baginski**	*Structure-Metabolism Relationships of 4-Pentenyl Synthetic Cannabinoid Receptor Agonists* ***(LRCFS)***
1020 – 1040	**Corrina Wilson**	*Exploring age-related trends in cortical and trabecular bone in an elderly Scottish sample: a pilot study on the clavicle* ***(CAHID)***
1040 – 1100	**Mohamed Ahmed**	*Ink formulation and printing of electrolyte for a doped ceria solid oxide fuel cell* ***(Phys)***
1100 – 1120	**Coffee break** (Dalhousie Foyer)	
Session 6	Chair: Vladimir Janjic + PGR (Dalhousie Lecture Theatre 2)	
1120 – 1140	**Thomas Riccio**	*A versatile instrument for studying soil-structure interactions* ***(Civil)***
1140 – 1200	**Richard Harries**	*Assessing the Impact of Anabolic Androgenic Steroids on Drug-Drug Interactions: In-Vitro Evaluation of Metabolic Clearance of Common Illicit and Medicinal Compounds* ***(LRCFS)***
1200 – 1220	**John Paul Nwigwe**	*Neural Network Arbitration Congestion Control System* ***(Comp)***
1220 – 1340	**Lunch and poster session** (Dalhousie Foyer)	
Session 7	Chair: Andrei Pisliakov + PGR (Dalhousie Lecture Theatre 2)	
1340 – 1400	**Han Li**	*Evaluation of 0.22MHz to 1MHz focused ultrasound transducer performance through cranial bone* ***(Biomed)***
1400 – 1420	**Ikenna Ikele**	*Analysis of the cervical spine morphometrics and dynamic changes of the ligamentum flavum in Thiel bodies* ***(CAHID)***
1420 – 1440	**Yazhmozhi Vasuki Murugesan**	*Spell checker and suggestion generator for the Tamil language* ***(Comp)***
1440 – 1500	**Coffee break** (Dalhousie Foyer)	
Session 8	Chair: Alan Cuthbertson + PGR (Dalhousie Lecture Theatre 2)	
1500 – 1520	**Kieran Stuart**	*X-ray emission models of young stars with multipolar magnetic fields* ***(Phys)***
1520 – 1540	**Filip Jovanovic**	*Periodic forcing of a chaotic fluid system* ***(Civil)***
1540 – 1600	**Fatih Tiras**	*DNA Methylation Analysis for Forensic Applications with Nanopore Sequencing* ***(LRCFS)***
1600 – 1620	**Martin Sanner**	Detecting Solar active regions using statistical analysis (**Math**)
1620	**Concluding remarks and close (Day 2) (Alan Cuthbertson)**	

1630 onwards	**Optional visit to Beer Kitchen (Innes and Gunn)**

Poster Presentations 1: 12:40 – 13:10, Thursday 11th May 2023

Presenter	Title
Saeed Charbenny	*Simulating the effect of a Single Element Focused Ultrasound Transducer various distances from skull* ***(Biomed)***
Andrew Dennison	*Can consumer desktop additive manufacturing produce reproducible microscale feature parts?* ***(Biomed)***
Matthew Eadie	*Investigating the limitations of endomicroscopy and how they can be improved* ***(Biomed)***
Jinpeng Liao	*A Deep Neural Network-based Method for Assessment of Wound Healing in Mice* ***(Biomed)***
Amirhossein Pourali	*Photoacoustic Microscopy Imaging* ***(Biomed)***
Daiyuan Xie	*The importance of Microfabrication in Healthcare: Enabling Personalized and Complex Medical Devices* ***(Biomed)***
Youheng Zeng	*Electrical impedance of an ultrasonic needle device as an indicator of needle tip position* ***(Biomed)***
Tianyu Zhang	*Development of a Handheld Swept-Source Optical Coherence Tomography System with High-Speed Acquisition* ***(Biomed)***
Morgan Hetherington	*Quantifying the impact of source variability on buoyant jet behaviour* ***(Civil)***
Yi Yuan	*Fluid-solid flow transitions in mixed (sand-mud) sediments: Enhanced modelling of sedimentation I estuarine and coastal waters* ***(Civil)***
Yimeng Wang	*Development and evaluation of antibacterial surfaces for medical implants* ***(Mech)***
Haoxuan Li	*Next Generation of RF Sensors for Digital Health Applications* ***(Mech)***
Zhengshuyi Feng	*Handheld probe design for internal cancer in Optical Coherence tomography based on Elastography* ***(Mech)***

Poster Presentations 2: 15:10 – 15:30, Thursday 11th May 2023

Presenter	Title
Jeffrey Anderson	*Cortical and trabecular bone ageing in the elderly: a 2D-3D approach on the rib and metatarsal* ***(CAHID)***
Kailey Lohmann	*Developing the standards used in facial approximation: a geometric morphometric of the eye across three populations: European, Arab and South Korean* ***(CAHID)***
Godfrey Inyama	*Dialogical Fingerprinting* ***(Comp)***
Somaye Moslemnejad	*How machine learning algorithms can analyse argument mining* ***(Comp)***
Nicole Orr	*Tools for Managing Argumentative Dialogue* ***(Comp)***
Elaine Scougal	*Exploring the use of AAC to facilitate the communication of children and young people with Down syndrome* ***(Comp)***
Chenyu Wang	*Multi-Modal Alignment for Radiology Report Generation Based on Conditional Reports* ***(Comp)***
Kathryn Burton	*Comparison of a newly developed fluorescent nanobioesensor to ion mobility spectrometry for the detection of cocaine* ***(LRCFS)***
Simon-Lewis Menzies	*Balancing The Scales of Justice: The Communication of Scientific Evidence and the Impact on Case Progression and Prosecution Decision-Making in Scotland since 2009* ***(LRCFS)***
Shen Hong	*Stability Analysis for Laminar Flows for Asymmetric Case* ***(Math)***

ORAL PRESENTATIONS

(In order of programme)

Developmental changes in the internal architecture of the human distal tibia

Rebecca Reid[1], Craig Cunningham[2], Catriona Davies[3]

[1] Centre for Anatomy and Human Identification, 110006554@dundee.ac.uk

[2] c.a.cunningham@dundee.ac.uk

c.m.davies@dundee.ac.uk

Abstract

Bones within the ankle joint play a significant role in weight bearing locomotion. However, there is a lack of knowledge regarding the impact of the changing biomechanical forces associated with the attainment of motor milestones upon these bones in juvenile humans. Analysis of these bones may have important clinical applications, in the treatment of paediatric trauma and therapeutic intervention of some pathological conditions. Therefore, the aim of this project was to investigate changes in the bone microarchitecture of the distal tibia through a variety of imaging techniques.

A novel combination of radiographic colour gradient mapping and radiographic absorptiometry was utilised to examine 96 human distal tibiae from 54 individuals ranging in age-at-death from 28 weeks intrauterine to 23 postnatal years. Radiographic colour gradient maps were placed in groups of shared morphology and radiographic patterns using an aluminium bone mineral density equivalents (Al BMDE) scale for reference. This qualitative analysis was complemented by microcomputed tomography of the distal tibiae for 34 individuals up to 9 years of age. Trabecular bone analysis, including quantification of bone volume fraction, degree of anisotropy, trabecular thickness, trabecular number and trabecular spacing, was conducted within 33 spherical volumes of interest in the distal tibia. Descriptive statistics for each developmental group identified during the radiographic study were applied to the preliminary microcomputed tomography results.

Radiographic and microcomputed tomography results both demonstrate distinct developmental phases within the juvenile tibia. At around the time of birth, tibial bone microstructure is dense with a high bone volume fraction. This gestational overproduction of trabecular bone is hypothesised to be in preparation for subsequent bone changes after birth. Between birth and two years of age, the tibia observes a period of constructive regression. During constructive regression, both radiographic and microcomputed tomography results indicate a decrease in bone quantity. This is postulated to be due to a combination of factors including changing locomotive forces, nutritional changes associated with weaning, and growth. After two years of age, the distal tibia demonstrated refinement where radiographic trajectories progressively developed into patterns consistent with the adult trabecular organisation, accompanied by an increase in several trabecular parameters. This refinement is consistent with increased structural organisation of the tibia to accommodate biomechanical forces associated with the bipedal gait.

Overall, qualitative and quantitative analysis of the juvenile tibia indicates the internal microstructure is influenced by biomechanical forces during development. Future work will include a closer examination of the structural heterogeneity with the tibia and will be extended to the talus, another bone within the ankle joint.

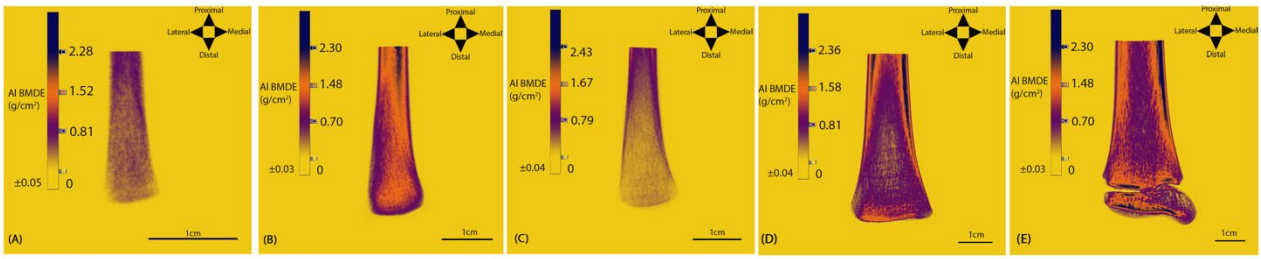

Figure 1: Radiographic colour gradient mapping of the developing juvenile tibia. A) Foetal; B) Birth– 6 months; C) Birth– 2 years; D) 2–10 years; E) 7–9years.

Effectiveness of Biometric Technology in the Context of an African Election: Investigating the Possible Causes of Fingerprint Verification Failures

Oluwafemi Samuel[1], Iain Martin[2], Ludovic Magerand[3]

[1] Computing, University of Dundee, o.a.samuel@dundee.ac.uk

[2] i.matin@dundee.ac.uk

[3] l.magerand@dundee.ac.uk

Abstract

The world today is moving away from conventional methods such as PINs and passwords to using biometric features for user authentication. In a bid to curb electoral fraud, African countries such as Ghana, Nigeria and Kenya have employed biometric verification as an integral part of their electoral processes for over a decade, initially with fingerprints but now introducing facial recognition also. While these countries have benefited from the transition from manual to electronic verification, the use of biometric technology during elections has not been without its challenges. Besides other technical problems, the failure of the fingerprint recognition technology to verify some electorates has been recorded across these countries at various elections. For instance, Kenya and Nigeria recorded fingerprint verification failure rates of about 4.6% and 10% during their elections in 2017 and 2019 respectively. Following the just concluded Nigerian elections, the European Electoral Observation Missions (EU EOM) reported that electoral officers opted to use facial recognition rather than the fingerprint component of their bimodal system, possibly because of recurrent issues of fingerprint verification during previous elections. Meanwhile, fingerprint recognition is expected to be more accurate, going by the required performance metrics of biometrics i.e. universality, distinctiveness, permanence, collectability, performance, acceptability, circumvention and cost. But where possible, improvement in the accuracy of fingerprint verification will ultimately improve the accuracy of the bimodal system. However, the desired improvement cannot be achieved without first identifying the causes of the fingerprint verification failures experienced.

The aim of this research is to investigate the possible causes of fingerprint verification failures at the elections in one of the African countries mentioned above – Nigeria. In doing so, fingerprint quality assessment (using a standard tool, NFIQ 2) has been conducted on sample fingerprints of some of the electorate in replica election settings. The fingerprint dataset and corresponding metadata being used for this research was newly collected and is to be published for research purpose. It comprises a total of 288 participants of age groups 18 (inclusive) to 99 years and over 12,000 fingerprint samples collected in Nigeria with various causative factors of verification failure incorporated.

An initial statistical analysis of the fingerprint quality assessment indicates that factors such as age, consistent placement of fingers on the scanner, physical condition of the fingertip (e.g. sweatiness vs dryness) are more likely to impact on verification than gender and occupation. Surprisingly, a t-test conducted (at α=0.05) shows no sufficient evidence to suggest that there is a statistically significant difference in fingerprint quality between electorate involved in manual work and those who are not. To further compliment the quality assessment analysis, experiments aimed at matching the fingerprints samples are ongoing. Because they have consistently remained benchmarks for assessment of fingerprint recognition algorithms, MinutiaeNet and Minutiae Cylinder Code (MCC) are being used for feature extraction and matching respectively. The analysis resulting from these experiments will be compared to that of the quality assessment for notable consistencies or disparities in findings. Comparisons will be made with findings from relevant literature also.

And the overall research output will inform recommendations to the EMBs, for improved accuracy of fingerprint verification in their subsequent elections.

Diagonally Scanned Airy Light-Sheet

Laurynas Valantinas[1], Tom Vettenburg[2], Michael MacDonald[3]

[1] Physics Department, University of Dundee, lvalantinas@dundee.ac.uk
[2] tvettenburg@dundee.ac.uk
[3] m.p.macdonald@dundee.ac.uk

Abstract

Light sheet microscopy has emerged as a powerful tool for high-speed, high-resolution imaging of fluorescent biological specimens, such as embryos, enabling the visualisation of dynamic processes of live tissue development with minimal phototoxicity. Instead of scanning the sample point-by-point, they illuminate a whole sample plane with a thin sheet of light, capturing the entire image plane in one shot in the normal direction of the plane.

However, light sheet microscopes' short depth of focus remains a limiting factor in their imaging capabilities, particularly when the light sheet is produced from a Gaussian beam. To address this limitation, researchers have developed techniques to scan with non-diffractive beams, such as the Airy beam, which extends the depth of focus by order of magnitude.

Airy beams possess the non-diffractive beam property of "self-healing" that enables them to compensate for scattering in embryos, allowing them to see deeper into the tissue. However, the detailed transversal structure of Airy beams, with multiple lobes of high light intensity, produces out-of-focus artefacts in scanned images. Deconvolution techniques are commonly used to remove these artefacts, but they are computationally demanding and typically limit the scanning geometries that can be used in light sheet microscopy. To account for the light-scattering nature of embryos and to capture their fast development, the light sheet must be scanned diagonally across the sample. This creates a challenge for typical deconvolution algorithms used for Airy beams.

We developed a new algorithm that enables fast deconvolution of diagonally scanned Airy beam light sheets. This allowed us to scan chicken embryos in diagonal geometry, keeping up with their rapid rate of development. Using the Airy beam as the basis for the light sheet, we were able to exploit the extended field of view and the “self-healing” properties of the beam. Our algorithm overcomes the computational demands of deconvolution and allows for real-time imaging of developing embryos with high contrast.

A review of lean communication practices for construction mega-projects in Saudi Arabia

Hussam Namanqani[1], Mr. Andrew Munns[2]

[1] University of Dundee, Civil Engineering, 2410561@dundee.ac.uk
[2] a.k.munns@dundee.ac.uk

Abstract

Over the past seven years, since the establishment of the national Vision 2030, Saudi Arabia has undergone a significant transformational period in its history. The construction of mega-projects has become a major facet of development within the country, but these have not been without their problems in failing to finish successfully either on time or within budget. As a consequence of this, construction mega-projects found their procedures and practice a significant challenge due to the pressure of new policies and waves of international competition. To assist stakeholders to achieve success on these projects an emphasis on the management of communication qualities and conflicts within project processes and phases is suggested. This could be achieved through employing lean thinking techniques, which were established to reduce waste and promote the performance of managerial practices on construction projects. For this to be successfully achieved on mega-projects, more needs to be learnt about lean thinking, its practices, challenges, and opportunities within the Saudi cultural framework. This paper aims to outline the possibilities for using lean thinking in overcoming communication conflicts on mega-projects through using of a systematic literature review (SLR).

The SLR was conducted on lean construction practices internationally and in KSA. Employing a structured search strategy seventy-seven articles were analysed and investigated for lean communication processes, drivers, and practices. The role of lean thinking and its tools for overcoming communication problems and partner conflicts are essential to identify better the source and causes of communication challenges and issues on mega-projects.

Themes and main ideas were extracted from the SLR, which included several essential variables, namely knowledge share, communication tools, and information flow in the construction mega-projects. The themes indicate the need for lean communication to support the transition between implicit and explicit knowledge through the three organisational levels of individual project members, working team, and leadership. The proposed conceptual framework that develops from these themes is a simple tool to describe a mechanism to allow information and knowledge to become visible and available for all stakeholders for better understanding and effective communication on mega-projects in Saudi Arabia, while following a lean thinking methodology.

Changing Trends in Benzodiazepine Use Within Scottish Prisons: Detection, Prevalence and Modes of Use

Victoria Marland[1], Dr. Herve Menard[2], Prof. Niamh Nic Daeid[3], Dr. Craig McKenzie[4]

[1] Leverhulme Research Centre for Forensic Science, University of Dundee, 2470848@dundee.ac.uk

[2] h.menard@dundee.ac.uk

[3] n.nicdaeid@dundee.ac.uk

[4] Chiron AS, craig.mckenzie@chiron.no

Abstract

Drug related deaths in Scotland are at their highest level since records began, doubling from 527 in 2013 to 1,339 in 2020. Polydrug use, where more than one drug are taken together, significantly contributes to drug harms and there has been a sharp rise in the availability and use of novel benzodiazepine type drugs ('street benzos'). Benzodiazepine-type drugs include diazepam (commonly known by its trade name Valium), etizolam and other related substances.

Drug use within prisons is increasingly complex, chaotic and unpredictable and many of the drugs used can be difficult to detect. Potent psychoactive substances can be infused into a range of materials and smuggled into establishments where they are vaped or ingested. The infusion of synthetic cannabinoids (SCRAs) into papers sent to prisoners via the mail system is an established smuggling method. Since late 2020, as a result of an extensive prison mail drug monitoring programme incorporating rapid on-site drug detection and laboratory-based analysis, we have identified increasing volumes of letters and textiles (Figure 1) infused with benzodiazepine type drugs.

Although the specific drug is commonly identified within seized samples by forensic laboratories, quantitative analysis is rarely undertaken. Therefore, the variability of drug content within and between dosage units remains mostly unknown, limiting our understanding of potential drug harms. Furthermore, changes in legislation can greatly impact the prevalence of the compounds detected, both locally and globally.

This work reports the qualitative detection, prevalence and emerging modes of concealment of benzodiazepine-type drugs detected within drug samples seized in Scottish prisons and describes the development of a quantification method for etizolam. Between February 2019 and January 2023, a total of 497 seized samples from 11 Scottish prisons, including paper, cards, blotters, powders, tablets and clothing, were analysed using Gas Chromatography-Mass Spectrometry (GC-MS). Throughout 2020/2021, Etizolam was the most commonly detected benzodiazepine type drug, however, following the international legislative control of etizolam in November 2020, the novel benzodiazepine detections became more diverse. As a result, by early 2023 a new substance, bromazolam, became the most prevalent benzodiazepine detected within this monitoring project. The concentration of etizolam was determined in 193 samples using GC-MS. Concentration mapping across an example greeting card (Figure 2) revealed the total concentration of drug present (312.5mg) and the variability measured across the card demonstrated the challenge of consistent dosing for users who will tear off pieces of card as individual dosage units. Increased understanding of the challenge of such drug smuggling and use helps inform strategies to reduce supply and mitigate harms.

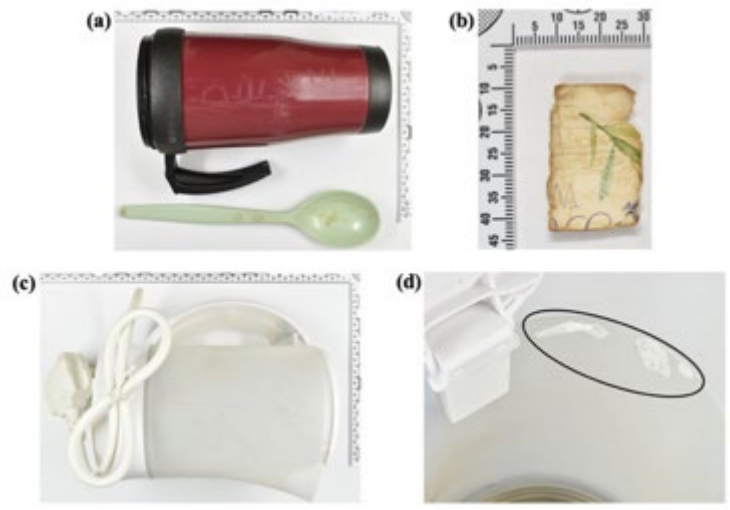

Figure 1: Examples of paper and card samples found within kettles and mugs: (a) FL21/0120: mug and spoon seized on 17th January 2021 with a piece of card inside (b) found to contain etizolam and the synthetic cannabinoid ADB-4en-PINACA; (c) FL21/0124: kettle seized on 11th February 2021 with 5 pieces of paper inside (d) found negative but presumed to contain novel benzodiazepines prior to extraction in the kettle.

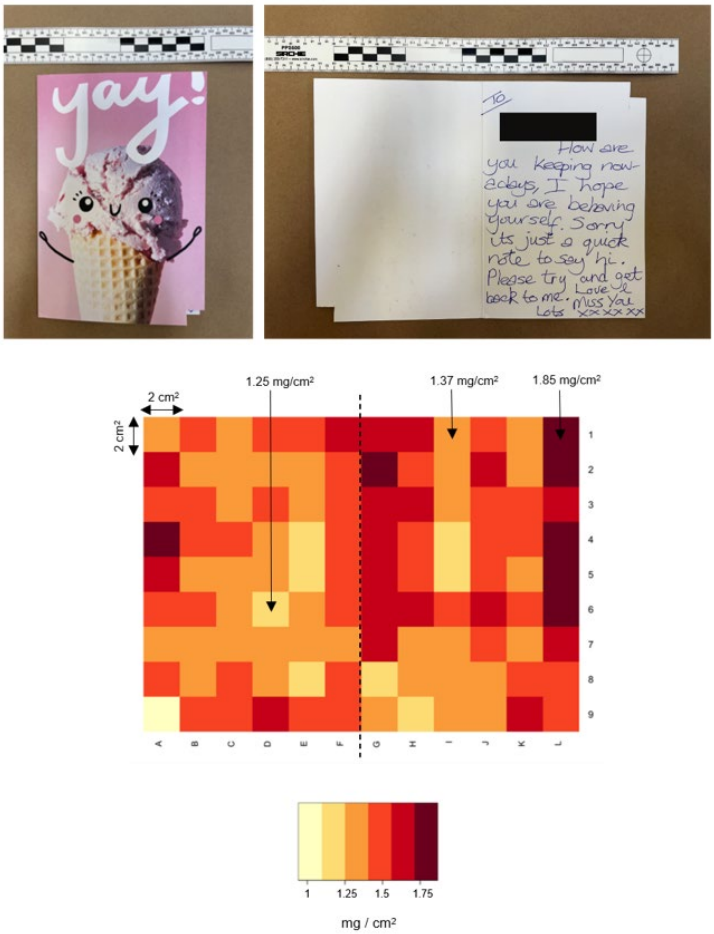

Figure 2: Concentration mapping of etizolam across a whole card sample.

Current Practice in Stature Estimation

Claire McIntosh[1], Dr Helen Langstaff[2], Dr Julieta Gomez Garcia-Donas[3]

[1] Centre for Anatomy and Human Identification, University of Dundee, c.v.mcintosh@dundee.ac.uk

[2] h.langstaff@dundee.ac.uk

[3] jgomezgarciadonas001@dundee.ac.uk

Abstract

Analysis of the morphology, condition and standard measurements of skeletal remains can be used to estimate the biological profile. There are four components, age, ancestry, sex and stature. Stature is calculated by either considering the bones which contribute to stature and correcting for soft tissue components of stature (anatomical method) or measuring a skeletal element and inserting the measurement into an equation expressing correlation to stature (mathematical method). Long bones, such as the femur give optimal results. An ideal method would provide a figure for living height from values derived from skeletal measurements; replicating these conditions is difficult.

The landmark papers defining the mathematical method were developed using height measurements taken on conscripts during World War 2 and the Korean War. These were then matched to skeletal remains on repatriation (Trotter and Gleser 1952; Trotter and Gleser 1958). The methodology of this work has been questioned (Jantz et al, 1995). The lack of applicability to other populations has also been highlighted (Wilson et al, 2010). It has been suggested that stature estimation is the least valuable aspect of the biological profile (Parsons, 2017) when used in the identification of unknown human remains. Stature is also calculated by archaeologists who use the values as measures of environmental conditions and population health (Fernihough and McGovern, 2015).

The current practice of stature estimation within the United Kingdom and Ireland was surveyed to understand current practice in stature estimation and its perceived value as a discriminator in identifying unknown human remains. This is part of a wider PhD topic which considers the value of stature (height) estimation in the identification of unknown human remains and the validity of the process.

A questionnaire survey was distributed to participants that perform stature estimation in the UK and Ireland through the mailing lists for the Royal Anthropological Institute and the Chartered Institute for Archaeologists. There were 16 responses which were grouped into forensic anthropology (7) and archaeology (9).

The forensic anthropology group evidenced higher levels of certification, while the archaeologists had more years of experience and a higher frequency of stature estimation each year. Respondents ranked stature as the least important part of the biological profile on four occasions and the second least important on 12 occasions. 12/16 respondents stated that they used the method developed by Trotter and Gleser (1952;1958) which was described as “the accepted standard”. Only three respondents referred to guidelines (Mitchell and Brickley, 2017; Buikstra et al, 1994). The forensic anthropology group quoted a wider range of literature, the most recent being a guideline published in 2017 (Mitchell and Brickley, 2017). 9/16 respondents had teaching commitments around stature, with comments indicating that they continued to base teaching on traditional methods.

The responses provided evidence about the validity of stature as a discriminator in the identification of unknown skeletal remains. Qualified and experienced practitioners rated stature of low value when compared to other aspects of the biological profile. The practitioners remained reliant on questioned standards from the 1950s which, it was commented, did not match current or archaeological populations. There was little acknowledgement of newer work or utilisation of guidelines, indicating that further research is needed to understand the status of the art of stature estimation in practice.

References

Buikstra, J.E., Ubelaker, D.H. (1994) *Standards for Data Collection from Human Skeletal Remains: Proceedings of a Seminar at the Field Museum of Natural History*. Fayetteville, Arkansas: Arkansas Archaeological Society.

Fernihough, A., McGovern, M.E. (2015) Physical Stature Decline and the Health Status of the Elderly Population in England *Economics and Human Biology,* 16: 30-44.

Jantz, R.L., Hunt, D.R., Meadows, L. (1995) The Measure and Mismeasure of the Tibia: Implications for Stature Estimation *Journal of Forensic Sciences,* 40(5): 758-761.

Mitchell, P.D., Brickley, M. (2017) *Updated Guidelines to the Standards for Recording Human Remains.* Reading, England: Chartered Institute for Archaeologists.

Parsons, H.R. (2017) *The Accuracy of the Biological Profile in Casework: An Analysis of Forensic Anthropology Reports in Three Medical Examiners' Offices* PhD Thesis. University of Tennessee.

Trotter, M., Gleser, G.C. (1952) Estimation of Stature from Long Bones of American Whites and Negroes. *American Journal of Physical Anthropology,* 10: 463-514.

Trotter, M., Gleser, G.C. (1958) A Re-evaluation of Estimation of Stature Based on Measurements of Stature Taken During Life and of the Long Bones After Death. *American Journal of Physical Anthropology,* 16: 79-124.

Wilson, R.J., Herrmann, N.P., Meadows Jantz, L. (2010) Evaluation of Stature Estimation from the Database for Forensic Anthropology. *Journal of Forensic Sciences,* 55(3): 684-689.

The Effectiveness of Blended Learning in Mathematics for Secondary School Students and their Teachers and Parents in Saudi Arabia

Nader Alharbi[1], Dr John McDermott[2], Prof. Keith Topping[3]

[1] University of Dundee, nalharbi@dundee.ac.uk

[2] j.z.mcdermott@dundee.ac.uk

[3] k.j.topping@dundee.ac.uk

Abstract

Great strides have been made across the globe in the development of effective teaching approaches and methodologies for improving the efficiency of the learning process and catering to students' diverse learning styles. Blended learning has emerged as a promising teaching approach, integrating online and face-to-face learning strategies to enhance learning outcomes. In Saudi Arabia, the Ministry of Education has introduced the Madrasati platform to support distance learning and achieve the country's economic and digital transformation goals. Despite the increasing popularity of blended learning, there is a dearth of research on the effectiveness of the platforms such as the Madrasati platform in a blended learning approach for mathematics education in secondary schools.

In this study, a systematic literature review was conducted on blended learning in secondary mathematics. After the inclusion and exclusion process, as shown in figure 1, the process involved identifying studies through databases, removing duplicates, screening titles and abstracts, and analysing full articles based on inclusion and exclusion criteria. The quality of the selected studies was then assessed based on research methodology and analysis, resulting in a reduced number of full-text papers.

This study aims to investigate the effectiveness of blended learning by using the Madrasati platform on students' mathematics performance and students, teachers, and parents' perceptions and acceptance of the platform. A mixed-methods research design was utilising to collect data, including open-ended questionnaires, semi-structured interviews, and analysis of students' final results from four secondary schools in Qassim city. The study sample includes male and female government secondary school students, their parents, and teachers from different socio-economic areas. This factor might influence the effectiveness of blended learning using the platform, which could be caused by the differences in the accessibility, motivation or other factors between these two areas, such as internet access, infrastructure, and income variation.

The Technology Acceptance Model (TAM) was employed to analyse the data and test hypotheses related to perceived usefulness, ease of use, and mathematics information quality regarding the Madrasati platform. The study aims to contribute to the growing body of knowledge on blended learning in mathematics and offer new insights into the Saudi Arabian context. The findings will be of significant value to the Ministry of Education in achieving its long-term goals of utilising the Madrasati platform to improve the classroom setting and enhance students' mathematics skills.

The study's outcomes will provide valuable insights to learning institutions that are striving to implement technology in the teaching and learning process. The study's results will also encourage other countries to adopt national learning platforms to ensure the continuity of education and mitigate the risks of educational losses in the future. In conclusion, this study contributes to the literature on blended learning and provides empirical evidence on the effectiveness of the platforms such as the Madrasati in a blended learning approach for mathematics education in secondary schools.

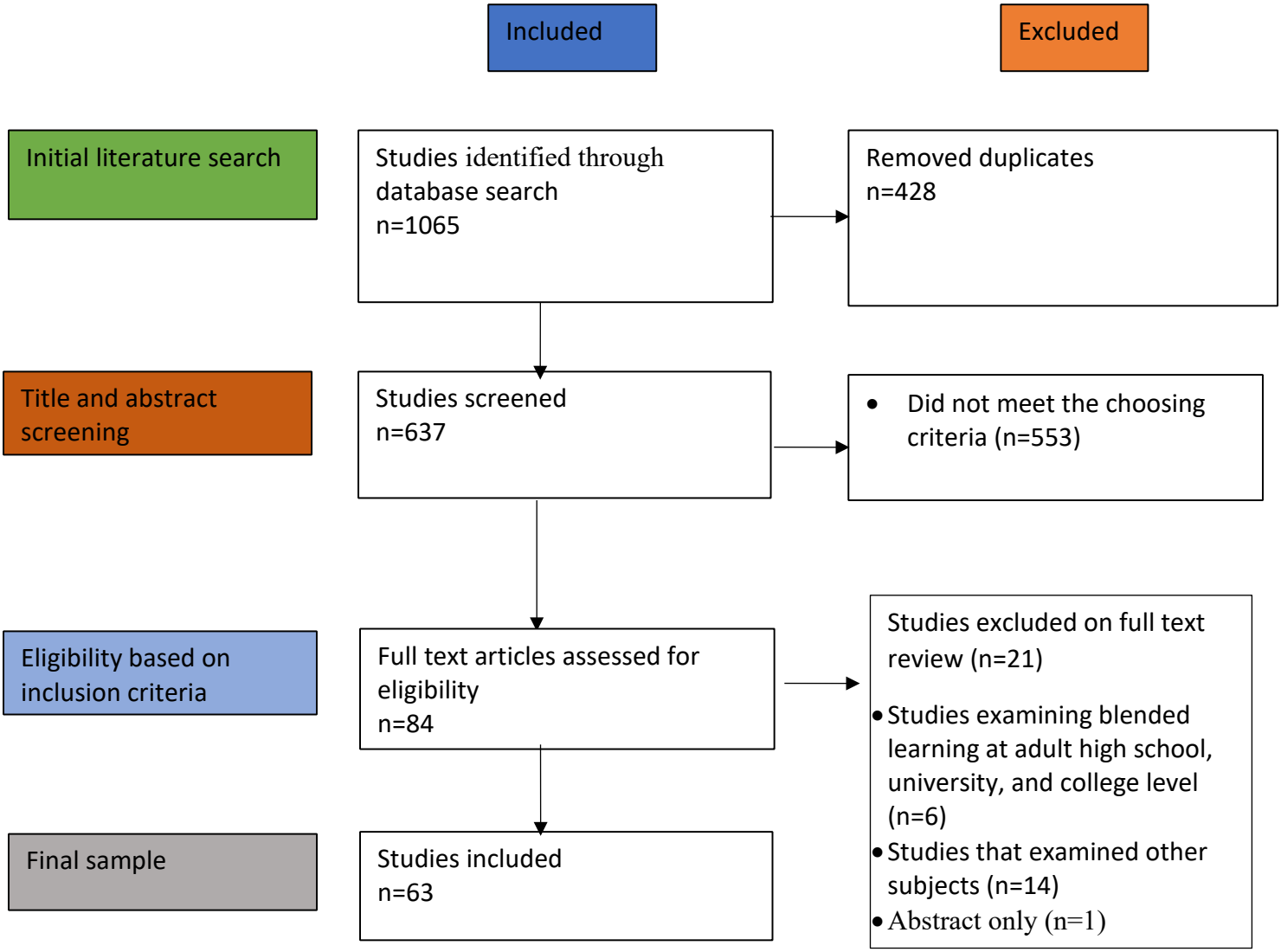

Figure 1: PRISMA Chart for Systematic Literature Review

Fairly and Rapidly Assessing Slowly Reacting Cement Concrete

Maciej Jozwik[1], Prof Rod Jones[2], Dr Moray Newlands[3]

[1] University of Dundee, mjozwik@dundee.ac.uk

[2] m.r.jones@dundee.ac.uk

[3] m.d.z.newlands@dundee.ac.uk

Abstract

Nearly 90 million tonnes of concrete are produced every year in the UK. Portland cement (PC) clinker production is a major source of CO_2 emissions, therefore, replacing PC by low carbon alternatives is the most promising path to reach the Government's net zero by 2050 target [1].

The development of low carbon concrete is probably the biggest and most important topic in the field of cement and concrete science and technology. There are myriad materials and solutions emerging that have specific characteristics suited to particular applications and regions depending on, for example, their local availability. In terms of large-scale concrete industrial output there is likely to always be a core of Portland cement clinker driving the reactions of much lower embodied energy cements and fillers. These will be familiar materials such as fly ash, ground granulated blastfurnace slag, limestone fines and, over the next decade, calcined clay as production begins at large scale.

Displacement of PC by up to 40% is not new, however, higher replacement levels of >50% are rarely utilised due to slow initial rate of hydration and associated increased curing requirements. Low carbon alternatives typically require anywhere between 90-180 days of curing to reach equivalent standard concrete 28-day maturity, according to Harrison [2]. Whilst this has significant implications for programming of construction work, it is also difficult to make material performance comparisons within timescales suitable for clients and designers to make decisions on material specification.

This research explores the use of low carbon cements to replace Portland cement in concretes currently used in the construction Industry. A number of concretes were cast (one reference; three low carbon cements) and water cured at 20°C and 50°C. Initial results concluded that approximately 12 days of elevated temperature curing returns the 90-day strength-based maturity equivalency to 90-day traditionally cured concrete (at 20°C), Table 1. This means that potentially, the timescales for durability performance testing of low carbon concretes can be significantly reduced making them more attractive to designers and specifiers.

Table 1 Compressive strength values for 90-day standard cured samples vs maturity equivalent samples cured at 50°C

Compressive Strength Results [MPa]			
water/cement ratio	**Cement Type**	**90-day Standard Curing (20°C)**	**12-day Accelerated Curing (50°C)**
0.4	**70% PC + 30% FA**	53.5	53.2
	50% PC + 35% GGBS + 15% LS	56.8	49.0
	40% PC + 45% GGBS + 15% LS	48.1	47.2
	40% PC + 20% FA + 40% GGBS	60.2	55.7
0.5	**70% PC + 30% FA**	38.3	41.5
	50% PC + 35% GGBS + 15% LS	47.4	40.7
	40% PC + 45% GGBS + 15% LS	41.6	37.9
	40% PC + 20% FA + 40% GGBS	44.0	39.7
0.6	**70% PC + 30% FA**	32.2	28.5
	50% PC + 35% GGBS + 15% LS	31.9	27.8
	40% PC + 45% GGBS + 15% LS	33.2	27.9
	40% PC + 20% FA + 40% GGBS	32.8	29.2

References

Mineral Products Association, “UK Concrete and Cement Industry Roadmap to Beyond Net Zero,” 2020

T. A. Harrison, “Specifying resistance against carbonation-induced corrosion by performance,” *Magazine of Concrete Research*, vol. 71, no. 7, pp. 341–348, Apr. 2019, doi: 10.1680/jmacr.17.00397.

Development and Evaluation of Ag-PTFE-TiO_2 Based Nano-composite Coatings for Preventing Catheter-Associated Infections

Yuhang Dong[1], Qi Zhao[2], Thomas Jones[3]

[1] Mechanical and Electronic Engineering, University of Dundee, 2494951@dundee.ac.uk

[2] q.zhao@dundee.ac.uk;

[3] t.d.a.jones@dundee.ac.uk

Abstract

Catheter-associated urinary tract infections (CAUTIs) account for 40% of all hospital-acquired infections and more than 1 million CAUTIs occur annually in the United States and Europe. CAUTIs leads to severe health complications and result in blockage of the medical devices and increased mortality.

Over recent decades, many attempts have been made to coat catheters with antibiotics, polymers or silver alloy to prevent CAUTIs, but only silver-coated catheters and certain antibiotics-coated catheters have entered clinical use, however, they have issues of poor durability, limited long-term efficacy and potential antibiotic resistance. Silver-coating limitations include dead bacteria strongly adhering and high coverage causing them to lose their anti-bacterial properties. Polytetrafluoroethylene (PTFE) has inherent non-stick properties and based on this, Qi Zhao et al (2019) developed an Ag-PTFE nanocomposite coating by incorporating PTFE nanoparticles into a silver matrix, combining the silver bactericidal properties and PTFE non-stick properties. The Ag-PTFE coated catheters are more effective than Ag-coatings against CAUTIs.

The addition of small amount of TiO_2 nanoparticles can significantly increase the coating's electron donor surface energy value (γ-) which is desirable for reducing adhesion (Chen & Zhao, 2011), and TiO_2 nanoparticles also exhibit synergistic antimicrobial efficacy with AgNPs, warranting an investigation into the inclusion of TiO_2. The aim of the research is to develop the novel Ag-PTFE-TiO_2 nano-composite coatings for catheters to further improve the anti-bacterial properties of Ag-PTFE coatings. The research focus on the achievement of the following specific objectives:

1) Calculate the optimal surface energy and the content of each component by the XDLVO theory.
2) Coat stainless steel sheets and urinary catheters with a layer of Ag-PTFE-TiO_2 nano-composite coatings.
3) evaluate the anti-stick and anti-bacterial properties of the coatings using the bacteria that frequently cause CAUTIs and compared with existing uncoated/coated catheters.
4) Characterize the surface properties of the coatings using SEM, AFM, XPS ,QCM-D300 and OCA-20 etc;
5) Evaluate anti-encrustation performance of coated catheters with in-vitro bladder models.

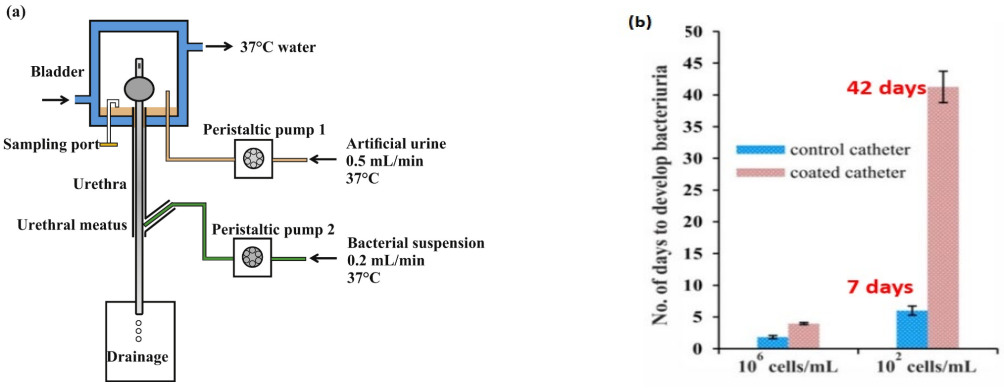

Figure 1: (a) Schematic diagram illustrating in-vitro bladder models to study bacterial migration along the surface of catheters; (b) Time taken to develop vateriuria of in-vitro evaluation of antibacterial performances of whole silicone (control) and Ag-PTFE nano-composite coated catheters using the bladder model.

References

Wang, L., Zhang, S., Keatch, R and Zhao Q. *et al*.(2019). In-vitro antibacterial and anti-encrustation performance of silver-polytetrafluoroethylene nanocomposite coated urinary catheters. *Journal of Hospital Infection*, 103(1):56-63.

Q. Zhao, Y. Liu, S. Wang, H. Müller-Steinhagen (2005), Effect of surface free energy on the adhesion of biofouling and crystalline fouling. *Chemical Engineering Science*, 60 (17):4858– 4865.

Chen Liu, Qi Zhao (2011), Influence of Surface-Energy Components of Ni–P–TiO2–PTFE Nanocomposite Coatings on Bacterial Adhesion. *Langmuir*, 27(15):9512–9519.

The Adventure of Argument: Narrative and Reasoning in Fictionalised Crime

Ella Schad[1], Chris Reed[2], Jacky Visser[3]

[1] Centre for Argument Technology, University of Dundee, e.m.schad@dundee.ac.uk

[2] c.a.reed@dundee.ac.uk

[3] j.visser@dundee.ac.uk

Abstract

Argumentation plays a critical role in the consumption of crime narratives. The public's unquenchable thirst for crime hasn't been slaked since the rise in the genre's popularity, providing a rich dataset through which to investigate the different kinds of reasoning (deductive, abductive, inductive) that play a role in the narratives of crime, as voiced by characters such as Conan Doyle's Holmes and Christie's Poirot. There is also argumentative tension between the red herring and the real culprit within the narrative; within other fictionalised environments, such as the films *Clue* and *Rashômon,* multiple competing hypotheses can be supported by evidence in the narrative. Investigation of the role of narrative within complex reasoning structures in fictionalised environments allows us to better understand the role argumentation plays and how it relates to the real world, by extending out into real-world cases where endings are not quite so neatly wrapped up. By mapping out evidence, their corresponding questions that attempt to verify the data, and including own reasoning, it all helps to build towards a case of better understanding the reasoning processes and, eventually, the ways in which this can be improved.

I am currently within the exploratory phase of my research, where I aim to gather as much data and context as I can before delving into the substance of what I'll be doing. My future plans for my research revolve around my interest to help to direct the user towards the "correct answer": using available data to make concrete assumptions about future events or answer questions not yet answered. Whilst I am currently working within a low-stakes environment, it is one that allows me to focus on the narratives of evidence and creates a stable platform within which I can play around with data. My research will, in the future, branch out into the "real world" where I can use real data to further these ideas and practices.

Structure-Metabolism Relationships of 4-Pentenyl Synthetic Cannabinoid Receptor Agonists

Steven Baginski[1], Lorna Nisbet[2], Craig McKenzie[3], Henrik Green[4]

[1] Leverhulme Research Centre for Forensic Science, University of Dundee 2470295@dundee.ac.uk

[2] lnisbet001@dundee.ac.uk

[3] c.t.mckenzie@dundee.ac.uk)

[4] Division of Clinical Chemistry and Pharmacology, Department of Biomedical and Clinical Sciences, Linköping University, Department of Forensic Genetics and Forensic Toxicology, National Board of Forensic Medicine, Sweden, henrik.green@liu.se

Abstract

Forensic toxicology involves the qualitative and quantitative analysis of drugs in biological samples and interpretation of the results, for legal purposes. A major challenge in the field in the last 15 years has been the significant rise in the number of new psychoactive substances (NPSs) detected on the illicit drug market, including synthetic cannabinoid receptor agonists (SCRAs). SCRAs bind to and activate the cannabinoid receptors, giving rise to similar effects to Δ^9-tetrahydrocannabinol (Δ^9-THC), the main psychoactive component of cannabis. However, SCRAs are significantly more potent and are associated with a greater number of adverse outcomes, including intoxication and death. SCRAs are constantly evolving as producers make new compounds to evade newly introduced legislation. Additionally, the rapid and extensive metabolism of SCRAs makes their detection in biological samples challenging, as the parent compound may be present only in low concentrations, especially in urine samples. *In vitro* metabolite identification studies are therefore essential in providing analytical targets to prove SCRA intake in clinical and forensic toxicology casework. Systematic studies on whole groups of SCRAs, in which small structural modifications have been made, can allow structure-metabolism relationships (SMRs) to be identified, which may help predict metabolites of emerging and future SCRAs.

In the presented study, the metabolism of a series of 4-pentenyl SCRAs was investigated *in vitro* to identify SMRs. The oxindole hydrazide BZO-4en-POXIZID and the (*S*)-enantiomers of 10 amino acid-derived SCRAs (AB-4en-PICA, AB-4en-PINACA, ADB-4en-PICA, ADB-4en-PINACA, EMB-4en-PICA, EMB-4en-PINACA, MMB-4en-PICA, MMB-4en-PINACA, MDMB-4en-PICA and MDMB-4en-PINACA) were incubated with pooled human hepatocytes for up to three hours. Metabolites were then identified using liquid chromatography–quadrupole time-of-flight mass spectrometry (LC-QTOF-MS). SMRs were examined by calculating the percentage that each biotransformation contributed to the total abundance of metabolites for each compound. Metabolites were mainly produced *via* dihydrodiol formation, terminal amide/ester hydrolysis and hydroxylation, but also by ketone formation, *N*-dealkylation, dehydrogenation, glucuronidation, and combinations thereof. Clear SMRs were identified. The ester hydrolysis products were the major metabolites for methyl-valinate (MMB) and ethyl-valinate (EMB) SCRAs (89.2% to 95.1%), whilst *tert*-leucinate (MDMB) SCRAs underwent less ester hydrolysis (48.5% to 62.0%) than MMB SCRAs, likely as a result of the extra methyl group increasing steric hindrance and thus reducing interaction with metabolising enzymes. The greater stability of amides to hydrolysis compared to esters resulted in a lower percentage of terminal amide hydrolysis for *tert*-leucinamide (ADB) and valinamide (AB) SCRAs (0% to 79.9%), and hydroxylation was the major metabolic pathway for ADB SCRAs. Dihydrodiol formation was most significant for SCRAs lacking a terminal amide or ester moiety (BZO-POXIZID: 61.5%), or in SCRAs which are more stable to hydrolysis of these moieties (AB, ADB and MDMB: 23.4 % to 36.0%). This knowledge will be used to aid prediction of metabolites of emerging and prophetic SCRAs.

Exploring age-related trends in cortical and trabecular bone in an elderly Scottish sample: a pilot study on the clavicle.

Corrina Wilson[1], Julieta Gomez Garcia-Donas[2], Craig Cunningham[3]

[1]Centre for Anatomy and Human Identification, University of Dundee, c.z.z.wilson@dundee.ac.uk

[2]jgomezgarciadonas001@dundee.ac.uk

[3]c.a.cunningham@dundee.ac.uk

Abstract

The human lifespan is increasing globally, increasing the need for further research on age-related changes in the bone of elderly individuals. Microscopic assessment of the skeletal system can provide information about the composition, mechanical, and functional properties of bone. The aim of this study is to combine 2D and 3D approaches examining cortical and trabecular bone to explore histological age-related changes in the clavicles of an elderly Scottish population.

The medial portion of 30 left clavicles was collected from Scottish donors from the Centre of Anatomy and Human Identification. The sample had a mean age of 83 years, with a sex distribution of 15 males and 15 females. Histomorphometric variables from the trabecular and cortical bone were collected. Five trabecular parameters were assessed using micro-CT scanning on two volumes of interest (VOI-superior and inferior sampling locations on the medial clavicular end). On the cortical bone, fourteen parameters were evaluated using traditional histological techniques. Cortical area related parameters were assessed on the whole cross-section, while osteon frequency related variables were measured on 8 sampling areas targeting key anatomical locations on the periosteal section of the clavicle.

Intra-observer error was assessed using intra-class correlation coefficient. The two VOIs were compared for statistical differences using paired t-test or Wilcoxon signed-rank test. Pearson and Spearman correlation coefficients were calculated, and age group comparisons were conducted for all parameters on the entire sample, the sample divided by decades (70s, 80s, and 90s), and the sample divided into two age groups (over/under 85 years). Sex differences were explored using an independent t-test and Mann-Whitney test. Lastly, stepwise regression analysis was used to test the optimal combination of parameters that could explain the highest variation in age.

Intra-observer error demonstrated overall good reliability for most parameters. Only bone volume fraction did not differ between VOIs, with all other trabecular parameters showing statistically significant differences. Cortical area parameters (cortical area and relative cortical area), intact osteon number, and both VOIs for trabecular connectivity density were statistically significantly correlated to age. When the sample was split into decades, no significant changes were observed over the three decades for cortical bone parameters (70s, 80s, and 90s). However, trabecular thickness and bone volume fraction differed statistically between individuals in their 70s and 80s. When the over/under 85 years groups were compared, only relative cortical area was statistically different between the two groups. Sex differences were found for cortical area related parameters (total area, endosteal area, and cortical area). Stepwise multiple linear regression showed that relative cortical area and inferior trabecular connectivity accounted for 30% of the variation in age.

This research showed that combining both cortical and trabecular bone using histomorphometric parameters can provide valuable information about age-related changes, suggesting also that other factors such as sex or age-related pathologies might have an impact on the changes observed in the two bone tissue types. While further research is necessary, this study adds to the growing research on bone histology using different populations and exploring the ageing patterns of an elderly population.

Ink formulation and printing of electrolyte for a doped ceria solid oxide fuel cell

Mohamed Ahmed[1], Thomas D. A. Jones[2], Amin Abdolvand[3]

[1] University of Dundee, m.m.s.m.ahmed@dundee.ac.uk
[2] t.d.a.jones@dundee.ac.uk
[3] a.abdolvand@dundee.ac.uk

Abstract

Fossil fuels used in electrical power stations are a major contributor to polluting carbon emissions and the resulting adverse effects of climate change prevalent today. Solid Oxide Fuel Cells (SOFCs) can produce electricity in a clean and sustainable way, and are thus a viable means of electrical power generation that has recently become an active field of research. A SOFC is an electrochemical energy conversion device that converts the chemical energy of hydrogen gas directly into electrical energy without combustion, giving off pure water vapour only. Thus, SOFCs are capable of addressing low-carbon emission targets by providing the generation of heat and power whilst utilizing sustainable and renewable sources, such as green hydrogen, and emitting water as refuse.

The development of these devices is hindered by high material costs and device degradation. Inkjet printing is a non-standard SOFC manufacturing technique which can address high material costs by reducing the required input material whilst providing high process reproducibility and speed compared with other SOFC manufacturing techniques, such as tape casting, nanolithography and atomic layer deposition techniques.

A simple ink formulation and a rapid preparation technique were proposed to deposit a nickel-cermet anode functional layer (AFL) ink and a gadolinium-doped ceria electrolyte ink utilizing micro- and nanopowders dispersed in a polymeric dispersant. The inks were assessed for printability by studying their rheology and calculating their Z-numbers. Subsequently, a drop-on-demand piezoelectric inkjet printer was used to deposit the gas diffusion electrode and electrolyte materials on a tape-cast anode support substrate. Ink drops are ejected only where required, thus keeping waste at minimal level. High quality jetting of SOFC inks is attained using inkjet piezoelectric printers owing to their flexible programmability providing full control over their cartridge's ejection voltage-waveform. Combined with proper adjustment of the size of the solid particles suspended in the ink using ultrasonication, this will prevent nozzle clogging and will allow for uniform printing. Additionally, the selection of a suitable ink dispersant will prevent the aggregation of the solid particles in the ink suspension, thus ensuring long-term ink stability. Polyvinylpyrrolidone (PVP) is a suitable candidate; an amphiphilic dispersant that is non-toxic to the environment, and also acts as a complexing and wetting agent.

A cost-effective 20 mol% gadolinium-doped ceria (20GDC) electrolyte ink and a Ni-GDC AFL ink were formulated based on a hybrid aqueous ethanol blank solvent complex (water as a solvent and pure ethanol as co-solvent) for a PVP dispersant. The resulting blank ink was solid-loaded with a 20GDC nanopowder for electrolyte and Ni-GDC micropowder for AFL, and ejection and printing were demonstrated. The ejected drops were investigated using printer built-in stroboscopic imaging during ejection (Figure 1), and the deposited thin films were characterised using optical microscopy and surface profilometry. Inkjet material deposition provides a highly repeatable process for the fabrication of solid oxide fuel cells (SOFCs) that can be up-scaled to industrial levels.

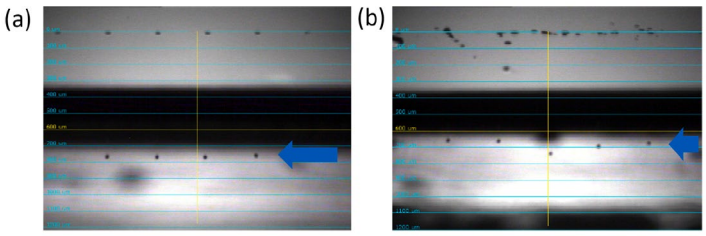

Figure 1. (a), (b) Stroboscopic 100 µs images showing ejected drops in-flight (by arrows) for the blank and solid-loaded inks respectively.

University of Dundee

A versatile instrument for studying soil-structure interactions

Thomas Riccio[1], Matteo Ciantia[2], Michael Brown[3]

[1] University of Dundee, 140007677@dundee.ac.uk

[2] m.o.ciantia@dundee.ac.uk

[3] m.j.brown@dundee.ac.uk

Abstract

Full scale testing of geotechnical problems (e.g., foundation installation and loading, embankment monitoring, drag anchor installation) can offer critical understanding of real-life performance. Full-scale modelling is, however, expensive, time consuming and often prohibitive due to the size and the forces required. Instead, carefully scaled model tests can be performed to offer valuable information on mechanisms of soil-structure interaction, as demonstrated by others, e.g., small scale studies of pile installation and lateral loading (Alvarez-Borges, 2019; Frick & Achmus, 2021). Recently, Riccio et al. (2023) used X-ray computed tomography to study lateral pile deformation of jacked piles (see Figure 1a) in an artificial porous rock (Jones & Mccarthy, 2005; Propump Engineering Ltd, 2003), which had similar characteristics to calcarenite. The post-test XCT offered an insight into the pile's plastic deformation after an applied lateral load which allowed for comparison of existing empirical and new numerical methods to inform the piles' hinge and head response (see Figure 1b).

In this work, a new standalone compact multi axis frame recently developed, fabricated, and operated to study geotechnical problems at 1***g*** is presented. The frame, instrumented with load cells and displacement sensors can apply coupled vertical and 2-way horizontal monotonic or cyclic load/displacement to a structure installed in a specimen (sized between Ø 100 mm - 300 mm). Actuation is mobilised by 7 DC motors and controlled using PID feedback. Its compact size allows the study of the soil/structure behaviour in-situ using μ-CT, whilst remaining under-load, overcoming the limitations of the original tests performed by Riccio et al. (2023) (see Figure 2a).

In this scope, focus is drawn to a series of tests performed within a XCT bay on small scale open-ended piles installed and laterally loaded in various geomaterials (see Figure 2b). It is shown that μ-CT can expose various geotechnical phenomena associated with pile installation. Imaging analysis is used to track pile behaviour (deflection) under a lateral load and subsequently the bending moment of the pile and lateral soil resistance, bypassing the requirement for local instrumentation (e.g., strain gauges) are often damaged during testing and challenging to interpret. Finally, following testing, higher resolution 3D-reconstructed tomography is used to study at the grain level material evolution induced by the installation and pile loading, such as densification and gapping around the pile perimeter.

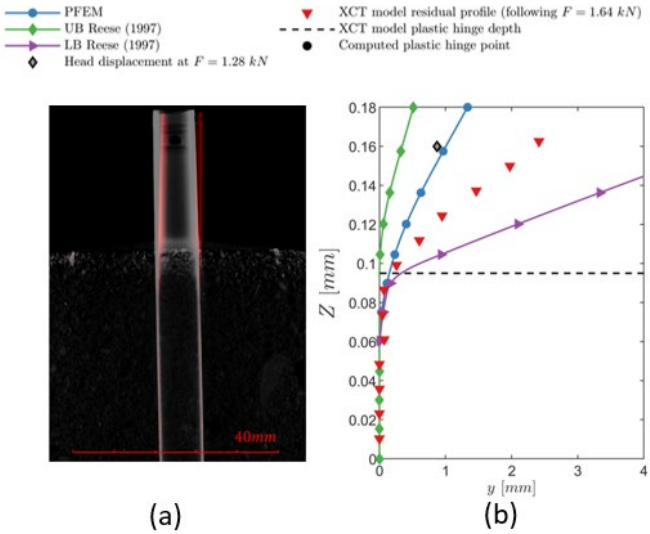

Figure 1: Small scale pile installed in an artificial porous rock and subject to lateral load (Riccio et al., 2023) showing a) XCT obtained pile deflection b) XCT deflection profile compared to predicted deflection profile through various lateral pile design

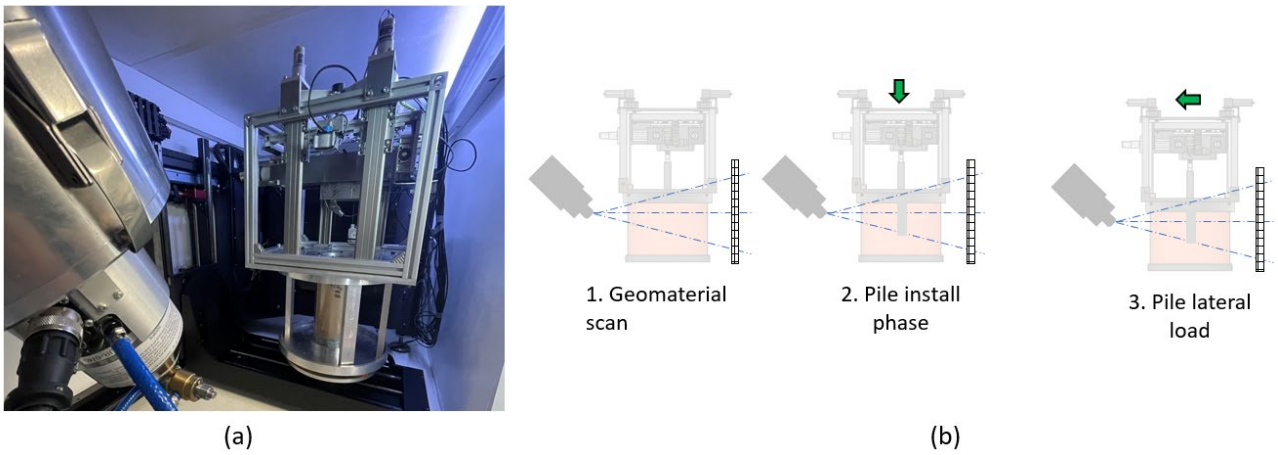

Figure 2: a) Multi-axis frame fully constructed and shown inside CT scanner performing a pile penetration test on sand b) Scanning and testing phases considered throughout the test phase

References

Alvarez-Borges, F. J. (2019). *The Shaft Capacity of Small Displacement Piles in Chalk* [Doctoral thesis, University of Southhampton]. https://eprints.soton.ac.uk/438900/.

Frick, D., & Achmus, M. (2021). A model test study on the parameters affecting the cyclic lateral response of monopile foundations for offshore wind turbines embedded in non-cohesive soils. *European Academy of Wind Energy (Wind Energy Science Discussions)*, *November*, 1–25. https://doi.org/10.5194/wes-2021-129.

Jones, M. R., & Mccarthy, A. (2005). *Preliminary views on the potential of foamed concrete as a structural material*. *1*, 21–31.

Propump Engineering Ltd. (2003). *Foamed concrete Strength vs density for different curing periods [confidential]*. Propump Engineering Limited.

Riccio, T., Previtali, M., Ciantia, M. O., & Brown, M. J. (2023). P-y response in porous rock : numerical derivation with experimental validation (under review). *9th International SUT OSIG Conference "Innovative Geotechnologies for Energy Transition."* https://sut.org/event/osig2023/.

Assessing the Impact of Anabolic Androgenic Steroids on Drug-Drug Interactions: *In-Vitro* Evaluation of Metabolic Clearance of Common Illicit and Medicinal Compounds

Richard L. Harries[1], Lorna A. Nisbet[2], Giorgia De Paoli[3], Andrew M. Brandon[4], Sarah Hall[5]

[1] Leverhulme Research Centre for Forensic Science, University of Dundee, 2518359@dundee.ac.uk

[2] lnisbet001@dundee.ac.uk

[3] g.depaoli@dundee.ac.uk

[4] abrandon001@dundee.ac.uk

[5] Health and Life Sciences, Leicester School of Pharmacy, De Monfort University, sarah.hall@dmu.ac.uk

Abstract

Background/Introduction: Drug clearance plays a vital role in determining the efficacy and safety of a drug, and can be influenced by drug-drug interactions (DDIs). DDIs occur when multiple drugs are present simultaneously in the body and the pharmacology of one or more is altered by another. Metabolic DDI can occur through various mechanisms, including competition for, or inhibition of, metabolic enzymes or transporters responsible for drug clearance and distribution. This can result in slowed drug clearance or altered metabolite formation. Illicit use of anabolic androgenic steroids (AASs) has increased in recent years, including polydrug use with cocaine and MDMA. AAS misuse has been linked with greater psychopharmacological treatment, while recent research has also detected the presence of AASs alongside synthetic cannabinoid receptors agonists (SCRAs). Currently there is a lack of information regarding the impact of DDIs on AASs and analyte clearance.

Objectives: To evaluate the impact metandienone, nandrolone and testosterone have on the metabolic clearance of ADB-FUBIATA, CH-PIATA, cocaine, MDMA, and quetiapine via *in-vitro* human liver microsome (HLM) incubations.

Methods: Intrinsic clearance of test compounds was measured in HLM incubations both with and without AASs. HLM (final concentration 0.5 mg/mL microsomal protein) solutions were prepared in potassium phosphate buffer (50 mM, pH 7.4) and, where appropriate, pre-incubated with each AAS (each at 10 µM) as potential inhibitors (5 min, 37 °C, shaking at 100 rpm). Test compounds and verapamil (positive control) (each at 0.5 µM) were added to incubations, and then 50 µL of NADPH (8 mg/mL) was used to initiate the reaction (final incubation volume 500 µL). Samples were incubated (37 °C, shaking at 100 rpm) and 50 µL samples were transferred to 200 µL acetonitrile (containing donepezil internal standard (IS) (10 ng/mL)) to stop the reaction at 0, 3, 6, 9, 15, 30, 45 and 60 min(s). Following incubation, 80 µL dH_2O was added to each sample before centrifugation (3750 rpm, 20 °C, 10 min). UPLC-MS/MS analysis was achieved by gradient elution using a Waters Acquity UPLC (column: Acquity BEH C18 (2.1 x 50mm, 1.7µm) coupled with a Waters Xevo TQ-S MS. Peak area ratio was plotted against incubation time to determine half-lives ($t_{1/2}$) and intrinsic clearance rates (CL_{int}) of parent analytes with and without the presence of AAS as potential inhibitors.

Results: Clearance of cocaine, MDMA and quetiapine were unaffected showing that their phase I metabolism by HLM is not significantly affected by the presence of these AASs. ADB-FUBIATA was also unaffected, however we can report here for the first time the experimental HLM clearance of this compound in isolation

($t_{1/2}$ = 9.82 ± 1.38 min). The intrinsic clearance of CH-PIATA was $t_{1/2}$ = 4.04 ± 0.47 min. CH-PIATA was found to be cleared at a slower rate in the presence of AASs, with CH-PIATA clearance as follows; with metandienone, $t_{1/2}$ = 12.42 ± 3.84 mins; with nandrolone, $t_{1/2}$ = 8.71 ± 2.56 mins; with testosterone, $t_{1/2}$ = 9.09 ± 2.48 mins.

Conclusion/Discussion: The co-incubation of metandienone with CH-PIATA resulted in, on average, a 3-fold reduction in CH-PIATA intrinsic clearance, while nandrolone and testosterone caused an average 2-fold reduction compared to CH-PIATA alone. This preliminary data suggests that high-dose AAS use may significantly affect CH-PIATA clearance *in vivo*.

University of Dundee

NEURAL NETWORK ARBITRATION CONGESTION CONTROL SYSTEM

JOHNPAUL NWIGWE[1], IAIN MARTIN[2], CRAIG RAMSAY[3]

[1] jnwigwe@dundee.ac.uk

[2] i.martin@dundee.ac.uk

[3] c.d.ramsay002@dundee.ac.uk

Abstract

TCP/IP is the backbone of packet switch network congestion control mechanisms. However, this control protocol is currently overwhelmed by the rapid increase of the Internet of Things. This has been the focus of many academic and industrial research. We propose a supervised learning congestion control mechanism called Neural -Network- multi-channel Routing congestion control system to address these challenges. Unlike the design of TCP/IP and its variants that rely on a slow start and congestion avoidance algorithm. The proposed model is designed to learn the traffic pattern and adjusts the size of the congestion window using the transmitting policy of the network topology to route packets to their destination. The feed-forward neural network is integrated into each node to optimize the routing decision by activating a channel that has free-slots for packet transmission after receiving feedback on each iteration on the queueing length (See, Fig 1). We generate packets whose source is randomly determined, Python and Keras frameworks are adopted for the implementation of the model and FFNN is trained based on the data obtained in simulations using a historical dataset obtained from a live data network company known as mobile telecommunication Company (MTN). An initial experiment was performed on the platform of a standard modern laptop without dedicated GPU support.

The result shows good classification accuracy between the input and output mapping sequence with high convergence speed and stable convergence process (See, fig2a & fig2b). The simulation results also show high bandwidth utilization and low congestion rate, indicating high throughput. Nevertheless, we intend to run further experiments to tune the algorithm based on a range of learning rate parameters to find the optimum value. The stability of the model will be analyzed with different network parameters of TCP/IP variants, bandwidth utilization, and target throughput.

Future work will include comparing our simulation with comparable research from recent literature using alternative network congestion algorithms on the same dataset to evaluate the effectiveness of our approach.

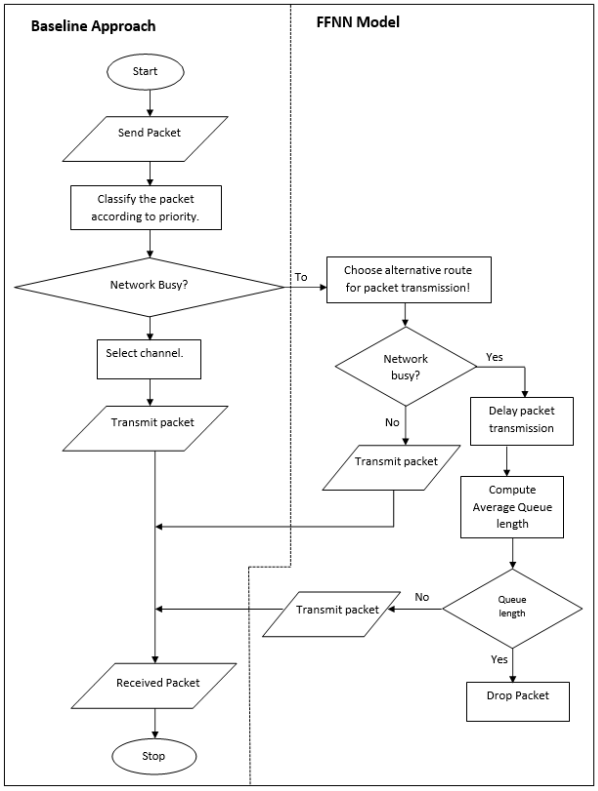

Fig1: Flowchart showing the relationship between the baseline method and learning-based model

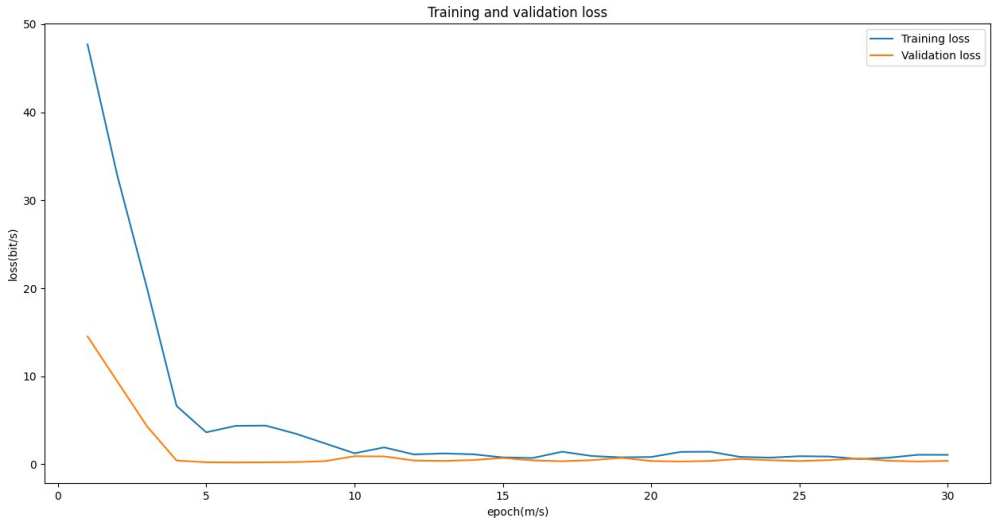

S/N	**Learning Rate**	**0.03**
1	Bandwidth Utilization	0.109 bps
2	Loss Rate After Training	0.0940079554494829
3	Packet Sent	5028 kbps
4	Packet Received	5019 kbps
5	Packet Retransmitted	9 kbps
6	Congestion Rate	4.209
7	Last Waits Time	5.307ms, 4.498ms, 7.180ms, 5.065ms
8	Network Efficiency	99%
9	Network Loss	0.01%
10	Classification Accuracy	1

Fig 2: (a) Test accuracy for the learning model, (b) Experiment 1 performance under 5 nodes at 5ms.

Evaluation of 0.22MHz to 1MHz focused ultrasound transducer performance through cranial bone

Han Li[1], Zhihong Huang[2], Andreas Melzer[3]

[1] University of Dundee, hwli@dundee.ac.uk

[2] z.y.huang@dundee.ac.uk

[3] a.melzer@dundee.ac.uk

Abstract

Objective: Transcranial focused ultrasound is established for applications such as thalamic ablation in the treatment of Parkinson's disease, blood-brain-barrier opening for drug delivery and deep brain stimulation. Low-intensity focused ultrasound (LIFU) is an emerging modality, able to reversibly neuromodulate neural circuitry. To achieve this, accurate transmission of a known dose of acoustic energy to the target brain area is required. This study aims to evaluate the performance of transcranial LIFU in the frequency range from 0.22MHz to 1MHz and to visualize the acoustic field at the focal point.

Methods: Four single-element focused ultrasound (FUS) transducers (Precision Acoustics, UK) with frequencies of 0.22MHz, 0.65MHz, 0.68MHz and 1MHz were tested. A needle hydrophone was mounted on a 3D positioning system to acquire acoustic data. In-house developed Matlab software was used for both scanning control, and data acquisition and processing. In total, 40 regions across 10 historical skulls were selected for testing. CT scans were performed to obtain density (and identify cavities). Speed of sound at each region was measured, and acoustic field maps (with time history) were constructed, which was sufficiently large to cover the signal amplitude higher than -6dB. 10V sinusoidal excitation was used across all experiments, which yielded approximately 0.2W of acoustic power.

Results: Insignificant focal point and phase aberrations were observed at normal incidence regions. Greater shifts were observed through regions of irregular curvature and thickness. Focal shift after adding the skull mostly within $(\pm 3, \pm 3)$mm. Although the acoustic reflection coefficient at the water-skull interface is typically at least 30%, by generating the standing waves between the skull and transducer, we achieved a minimum pressure loss compared to the free-field of 13% for the 0.22 MHz transducer. The effect of wave superposition decreases along the increase of the frequency, while the pressure variation at the in-phase and out-phase positions is still evident. The thickness of the skull is positively correlated with the attenuation of the pressure and focal intensity for all frequencies. The acoustic impedance is positive correlated for 0.22MHz while negative correlated to 0.65MHz-1MHz. This is evidence of lower frequency FUS is more efficient for penetrating spongy bone structures.

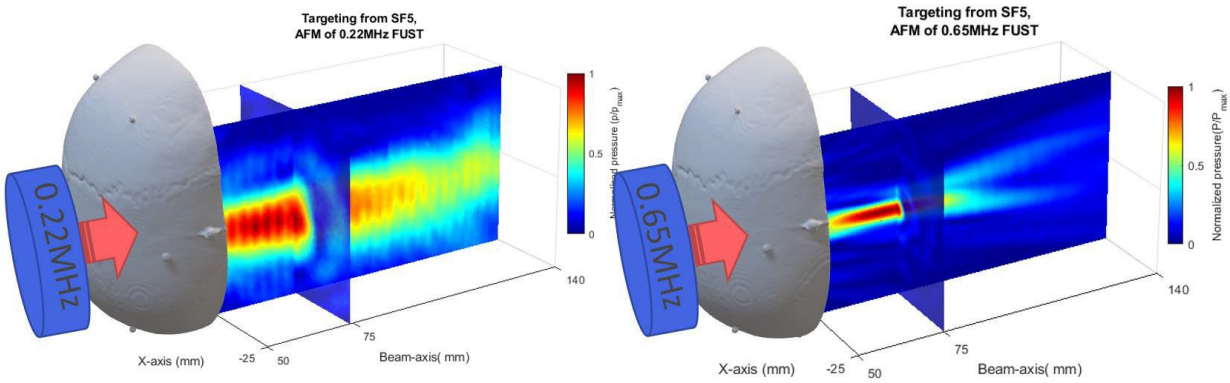

Figure 1: Acoustic field mapping with skull at 0.22MHz and 0.65MHz.

Analysis of the cervical spine morphometrics and dynamic changes of the ligamentum flavum in Thiel bodies

Ikenna T. Ikele [1], Seaneen McDougall[2], Kismet-Hossain Ibrahim[3], Tracey Wilkinson[4]

[1] Centre for Anatomy and Human identification, University of Dundee, i.t.ikele@dundee.ac.uk

[2] s.mcdougall@dundee.ac.uk

[3] School of Medicine University of Dundee, k.z.hossainibrahim@dundee.ac.uk.

[4] Human Anatomy Unit, University of Birmingham, a.t.wilkinson@bham.ac.uk

Abstract

Cervical spinal stenosis is caused mainly by degenerative changes and trauma that compress the spinal cord. Studies have suggested that 90% of individuals over the age of 60 will demonstrate some form of degenerative changes in the cervical spine region (Tykocki, *et al.,* 2018).

The loss of the elasticity of ligamentum flavum due to degenerative changes has been reported to be one of the probable causes of spinal stenosis, and its associated complications, due to increases in the thickness of ligamentum flavum, as well as buckling of the ligamentum flavum into the vertebral canal (Altinkaya *et al.*, 2011). Intervertebral disc height has been implicated to have a low to moderate correlation with the ligamentum flavum thickness (Munns *et al.*, 2015). Studies have also implicated the loss of disc height with age. This has important implications clinically and can be observed through plain lateral radiograph imaging (Tao *et al.*, 2021).

Cervical spinal stenosis is caused mainly by degenerative changes and trauma that compress the spinal cord. It has been known to occur most commonly in 90% of the older population (Tykocki, *et al*., 2018). The loss of elasticity of the ligamentum flavum due to degenerative changes has been reported to be one of the probable causes of spinal stenosis and its associated complications due to increased thickness of the ligamentum flavum and buckling into the vertebral canal (Altinkaya *et al.*, 2011). Intervertebral disc height has been implicated as having a low to moderate correlation with ligamentum thickness (Munns *et al.*, 2015). Studies have also shown the loss of disc height with age, which is of clinical importance and can be seen with a plain lateral radiograph (Tao *et al.*, 2021).

Cervical stenosis can also occur because of spinal stenosis- the condition whereby abnormal curvature of the spine can be seen. The degree of scoliosis can be calculated using the Cobb angle, as Zhang *et al.* (2018) discovered that the use of the Cobb angle is an effective tool in obtaining intra- and inter-rater reliability to determine cervical lordosis.

Currently, there is a paucity of information on how the morphometric parameters of the cervical spine and ligamentum flavum thickness may cause cervical stenosis. There is also a lack of information on the bony morphometrics of the cervical spine in a modern Scottish population.

This study therefore is a repeatable cross-sectional study that aims to correlate the bony morphometrics of the cervical spine (C3-C7) with the dynamic changes of the ligamentum flavum obtained through MRI as a potential predictor of cervical canal stenosis amongst the modern Scottish population. The various mean dimensions of the morphometrics of the cervical spine and the thickness of the ligamentum flavum will be calculated and compared to establish whether there are existing relationships between them, including age and sexual dimorphism.

Making use of MRI techniques, the project will then examine the thickness of the ligamentum flavum in flexion and extension positions in a subset of Thiel cadavers to see if any of these parameters correlate with the degree of cervical spine stenosis (obtained by measuring anteroposterior and medial-lateral canal diameter). Multiple bony morphometrics of the cervical spine will be directly measured to obtain normal confidence values for the modern Scottish population. The wider study will compare cervical morphometrics with ligamentum flavum thickness to explore whether specific morphological

characteristics correlate with thickness or Cobb angle. This has the potential to allow determination of a bony biomarker of canal stenosis (currently measurable only by MRI). The advantage might be that future studies could identify bony parameters that could be measured by plain radiographs, which would be a cheaper potential biomarker of cervical stenosis and a useful resource for low-income countries without MRI resources.

Technical and relative technical (TEM and rTEM) error of measurement will be calculated to check the repeatability of the measurements as well as comparing the measuring modalities. SPSS version 26.0 will be used for statistical analysis. P-values of <0.05 will be deemed statistically significant.

Key words: dynamic magnetic resonance imaging, Cobb angle, ligamentum flavum, cervical canal, disc height

References

Altinkaya, N. *et al.* (2011) 'Factors Associated With the Thickness of the Ligamentum Flavum: Is Ligamentum Flavum Thickening Due to Hypertrophy or Buckling?', *Spine*, 36(16), pp. E1093–E1097. doi:10.1097/BRS.0b013e318203e2b5.

Munns, J.J. *et al.* (2015) 'Ligamentum flavum hypertrophy in asymptomatic and chronic low back pain subjects', *PloS One*, 10(5), p. e0128321. Available at: https://doi.org/10.1371/journal.pone.0128321.

Tao, Y. *et al.* (2021) 'The impact of age, sex, disc height loss and T1 slope on the upper and lower cervical lordosis: a large-scale radiologic study', *European Spine Journal*, 30. Available at: https://doi.org/10.1007/s00586-021-06933-x.

Tykocki, T., du Plessis, J. and Wynne-Jones, G. (2018) 'Correlation between the severity of myelopathy and cervical morphometric parameters on dynamic magnetic resonance imaging', *Acta Neurochirurgica*, 160(6), pp. 1251–1258. doi:10.1007/s00701-018-3540-x.

Zhang, J. *et al.* (2018) 'Can C2-6 Cobb Angle Replace C2-7 Cobb Angle? An Analysis of Cervical kMRIs and X-rays', *SPINE*, 44, p. 1. Available at: https://doi.org/10.1097/BRS.0000000000002795.

Spell checker and suggestion generator for the Tamil language

Yazhmozhi V M[1], Annalu Waller[2], Jacky Visser[3]

[1] Computing, University of Dundee, 2473490@dundee.ac.uk
[2] a.waller@dundee.ac.uk
[3] j.visser@dundee.ac.uk

Abstract

A spell checker is software that checks for misspelled words and provides suggestions for them. Spell checkers are an important area in Natural Language Processing (NLP), improving the efficiency of machine translation, information retrieval, information extraction, etc and can also be integrated into word processing software and search engines. In addition, they can be of use to proof-readers, writers, students, and people with language disabilities like dyslexia. Tamil is an official language in Tamil Nadu, Pondicherry, Sri Lanka, and Singapore. It has 247 alphabets and is the mother tongue of more than 69 million people in India.

Three major types of errors occur in Tamil (see Figure 1). Non-word errors are invalid words that do not occur in the language. Real word errors occur due to contextual irrelevance. Sandhi errors occur when a vallina Mei letter is mistakenly added or dropped from the end of a word whose adjacent word begins with a vallina Uyirmei letter. 36 sandhi rules are identified: 18 for addition errors and 18 for deletion errors.

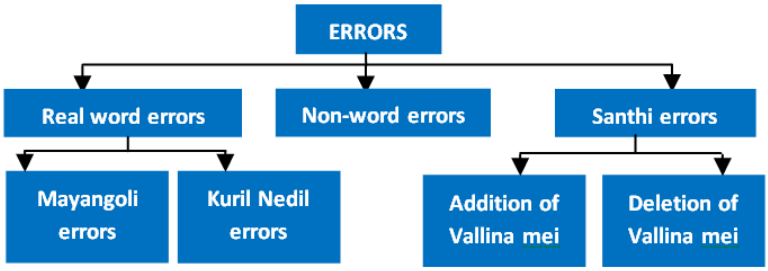

Figure 1: Types of spelling errors in Tamil

A systematic literature review of spell checkers for the major written Dravidian languages – Tamil, Telugu, Kannada, and Malayalam – has been conducted. An assessment of the quality of 56 relevant papers resulted in the analysis of 44 papers using twelve review questions. The research gaps and challenges highlighted the need for a Tamil spell checker that covers all types of errors. This research aims at the development of a spell checker and suggestion generator for the Tamil language that detects and provides suggestions for types of error specific to Tamil. The spell checker will also be designed to support Tamil writers who have dyslexia. Work is now underway to construct two unique Tamil language resources – a balanced Tamil written text corpus and a Tamil spelling error corpus. Nineteen genres – newspapers, letters, review articles, government reports, novels, short stories, other books, essays, Social Science, Science, Engineering, Finance, Religion, Law, Medicine, Mathematics, Arts, Research journals, and proverbs are identified for the construction of the balanced written text corpus. Proofread written Tamil text has been collected from most of these genres. A spelling error corpus will be constructed and published. It will serve as a benchmark corpus for the evaluation of the Tamil spell checker. The balanced written text corpus will be used to train the auto regressive and auto encoder language models to handle real word and non-word errors. The spelling error corpus will be used to do a comparative analysis of performance to find which model outperforms the rest. The techniques that will be used to handle the sandhi errors vary from rule to rule. Some rules are straightforward while others require ML/DL techniques. The techniques used for generating suggestions have also been identified and a method will be formulated to measure suggestion adequacy, a metric that computes the accuracy of the generated suggestions.

X-ray emission models of young stars with multipolar magnetic fields

Kieran Stuart[1], Scott Gregory[2], Karen Meyer[3]

[1] Physics, 2476691@dundee.ac.uk
[2] s.gregory001@dundee.ac.uk
[3] k.meyer001@dundee.ac.uk

Abstract

The behaviour of stellar X-ray emission changes throughout the lifetime of stars. This emission is a result of hot plasma confined along magnetic field loops in stars coronae. Stars of age of the Sun have much lower quiescent X-ray luminosities than that of young stars on the pre-main sequence (PMS) that have stronger magnetic fields which can contain plasma out to much larger scales. How X-ray luminosity evolves as PMS stars age is not well understood, partly due to the undergoing evolutionary changes in the stellar interior and global magnetic topology.

Many PMS stars have been observed to have simple and axisymmetric large-scale magnetic fields which can be well constructed from a magnetic field with a dipole and octupole component. Other PMS stars have large-scale magnetic fields that are complex and non-axisymmetric. Observations suggest that the complexity of the fields increases as stars evolve through the PMS (Gregory et al, 2012). For these stars it is also observed that X-ray luminosity decreases with age during PMS evolution (Getman et al, 2022). Together, these observations point to more evolved PMS stars with typically more complex magnetic fields tending to have lower X-ray luminosities.

We investigate how changes in the large-scale magnetic field topology of PMS stars influences coronal X-ray emission. The magnetic fields studied are axisymmetric multipole magnetic fields and magnetic fields consisting of a dipole plus an octupole component. For each system (for each magnetic field topology) we determine the closed coronal volume, within which X-ray emitting plasma is confined, using a pressure balance argument. The density over the coronal volumes is determined to calculate X-ray luminosities. We find that the stellar X-ray luminosity has a decreasing trend as fields become more complex. The X-ray luminosity values span over two orders of magnitude by varying the topologies in the cases considered when the stellar parameters are fixed. The trends found in this work reinforce the link between the increasing complexity of the large-scale magnetic field in ageing PMS stars and the decreasing X-ray luminosities in stars with age. Further analysis can be done to explore the behaviour of more complex, non-axisymmetric fields. Future works studying the evolution of X-ray behaviour with evolution on the PMS will include evolving stellar parameters based on evolutionary models, that consider the evolution of stellar rotation, magnetism, disc loss etc.

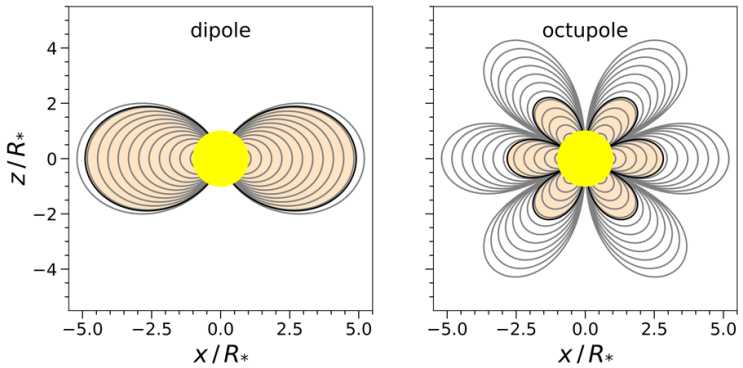

Figure 1: Magnetic fieldlines of dipole and octupole fields and the areas of enclosed plasma in beige.

References

Gregory S. G., Donati J. F., Morin J., Hussain G. A. J., Mayne N. J., Hillenbrand L. A., Jardine M. (2012), Can We Predict the Global Magnetic Topology of a Pre-main-sequence Star from Its Position in the Hertzsprung-Russell Diagram?, The Astrophysical Journal, 755, 97.

Getman K. V., Feigelson E. D., Garmire G. P., Broos P. S., Kuhn M. A., Preibisch T., Airapetian V. S. (2022), Evolution of X-Ray Activity in <25 Myr Old Pre-main Sequence Star, The Astrophysical Journal, 935, 43

Periodic forcing of a chaotic fluid system

Filip Jovanovic[1], Dr Tom S Eaves[2], Dr Alan Cuthbertson[3]

[1] University of Dundee, fjovanovic@dundee.ac.uk
[2] teaves001@dundee.ac.uk
[3] ajscuthbertson@dundee.ac.uk

Abstract

A significant challenge we are facing is the ever-growing demand for environmentally friendly and energy efficient transport as a result of emissions released from fossil fuels. A variety of approaches can be taken to optimise energy efficiency of transport and vehicles, one of which is to look at fluid flow drag reduction; surface drag (skin friction) plays a key role in causing unnecessary energy loss in vehicles. One potential method of reducing drag is to oscillate the surfaces of the flow transversely to the flow direction; simulations and experiments using this method lead to drag reduction of up to 25% (Quadrio, 2011), depending on the Reynolds number of the flow.

To better understand how such dramatic drag reductions can be made, we study the impact of the oscillatory forcing on simplified fluid systems using a dynamical systems approach. Specifically, we study the effect of periodic forcing on the long-term averages and structural properties of the famous Lorenz system which was originally derived as a simplified model of convection. It is well known that unstable periodic orbits play a key role in the dynamics of chaotic systems (Cvitanovic, 1991), forming the structure, or skeleton, of the attractor on which the chaotic trajectories evolve. As such, periodic orbits directly impact long-time averages in certain chaotic systems, and it is possible to compute average quantities of the chaotic motion using only properties of the orbits, including their period, stability, and average quantities measured on each orbit. This computation typically converges rapidly with the number of orbits used in a 'periodic orbit expansion' of averages of chaotic attractors (Cvitanovic & Eckhardt, 1991).

This presentation will detail the effect of periodic forcing on an average quantity of the Lorenz system (specifically a scaled heat-flux) along with the effect of this forcing on the unstable periodic orbits embedded within the Lorenz attractor. The ability of periodic orbit theory to predict averages in this oscillating system will be discussed, along with potential analytical tools (such as linear response theory) that will be developed to predict this behaviour a priori and hence deduce the response of chaotic fluid systems to oscillatory forcing using only properties of the unforced system. This work is helping to establish a mathematical framework with which to describe and explain the observed drag reduction and sets the groundwork for ongoing research into the effect of oscillatory forcing on the structures contained within the full Navier–Stokes equations. The ultimate objective of the project is to develop novel forcing techniques for drag reduction which lead to even greater savings, by understanding how structures within the fluid motion react to such forcing.

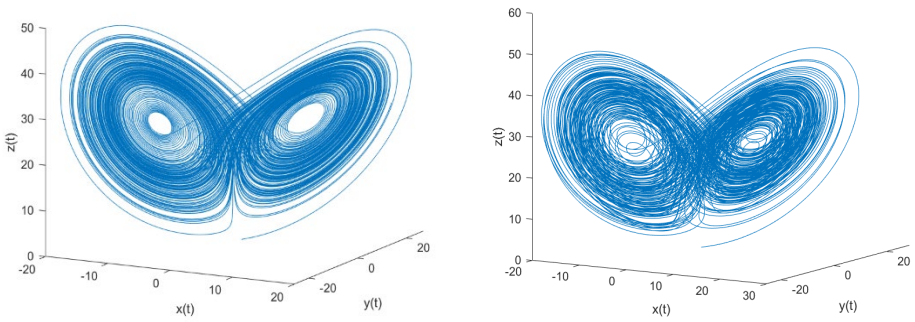

Figure 1: the attractor of left: the unforced and right: a forced Lorenz system.

References

Cvitanovic, P. (1991). Periodic orbits as the skeleton of classical and quantum chaos. *Physica D* 51(1-3): 138–151.
Cvitanovic, P. & Eckhardt, B. (1991). Periodic orbit expansions for classical smooth flows. *J Phys A* 24(5), L237.
Quadrio, M. (2011) Drag reduction in turbulent boundary layers by in-plane wall motion. *Phil T R Soc A* 369(1940), 1428–1442.

DNA Methylation Analysis for Forensic Applications with Nanopore Sequencing

Fatih Tiras[1], Dr. Alexander GRAY[2], Dr. Christian COLE[3]

[1]Leverhulme Research Centre for Forensic Science, University of Dundee, 2397405@dundee.ac.uk
[2] a.z.gray@dundee.ac.uk
[3]Health Informatics Centre, University of Dundee, C.Cole@dundee.ac.uk

Abstract

Forensic DNA analysis is an evolving technology, currently Short Tandem Repeat (STR)analysis is used in human identification. However, massively parallel sequencing (MPS) is now being used to extract more information from forensic DNA samples. This includes DNA modifications such as methylation which has been shown in certain genes to vary with age. This information would be useful in forensic investigations to give the approximate age of DNA donors at crime scenes and refugee age verification.

Traditionally methylation of DNA is detected by bisulphite sequencing where DNA is sequenced then bisulphite treated to convert methylated cytosine bases to thymine and resequencing conversion from C to T bases indicating the presence of methylation. We have used one of the latest MPS platforms, Oxford Nanopore Sequencing, which has the advantage that it can directly detect methylation of DNA without bisulphite treatment. This allows us to detect methylation at a genome wide scale since an entire genome can be sequenced with this technology in 48-72 hours.

The aim of this project is to provide proof of concept for this methodology and identify regions of the genome which vary in methylation content by age. We collected 24 buccal swabs were collected from volunteers with informed consent and ethical approval. DNA extraction and quantification were performed using Qiagen DNA extraction kit and Qubit respectively. Sequencing libraries were prepared and sequenced using Oxford Nanopore protocols.

The raw sequence data was analysed using a bioinformatics pipeline on the University of Dundee cluster system. The first step is generating the actual sequence of the DNA from the raw nanopore data this base calling process provides the template for the subsequent methylation analysis. Initially this analysis required 28 days per sample using CPU computation. However, further optimisation and using GPU computation this was reduced to 6 hours per sample. This allowed the assessment of 3 different DNA methylation determination packages, Meteore, Deepsignal and Nanopolish. To compare the outputs of these packages the data was visualised using the Methylartist package which generates graphical representation of the DNA methylation patterns. This has allowed analysis to be performed on all 24 samples 6 of which were eliminated due to sequence low coverage. 18 samples were selected for further analyses and this visualization program generated blocks of one million bases for the whole genome (Figure 1). Different regions were recorded by examining the graphics created. Then, these regions were examined more closely (Figure 2), and the different methylation distribution the samples showed was recorded. In future studies, whether these distributions correlate with the samples' ages will be investigated, and investigations are continuing.

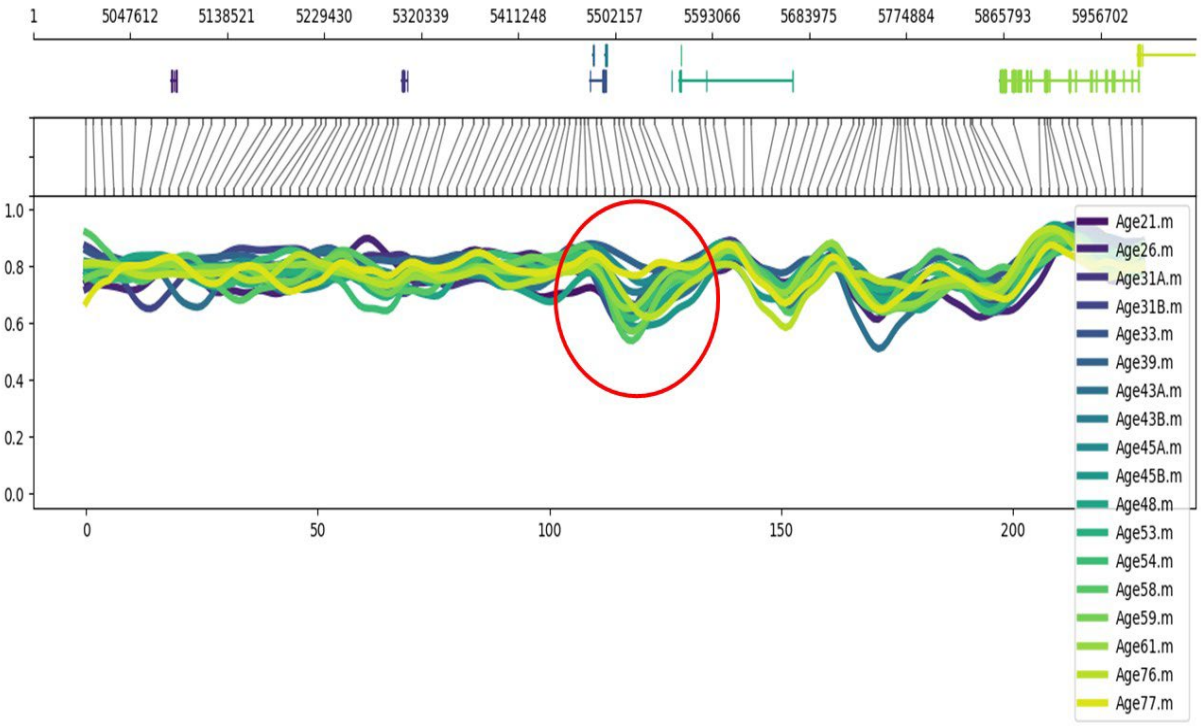

Figure 1: This plot shows a one million bp block from chromosome 1 (240 million bp) generated with the Methylartist methylation visualization package. The numbers on the top scale represent the location of the range in the genome. The coloured lines indicate the methylation ratio indicated on the y-axis different coulors indicate the age of the samples as indicated. Here, it is seen that the region shows a variation with age in methylation distribution around 5502157 bp (red circle).

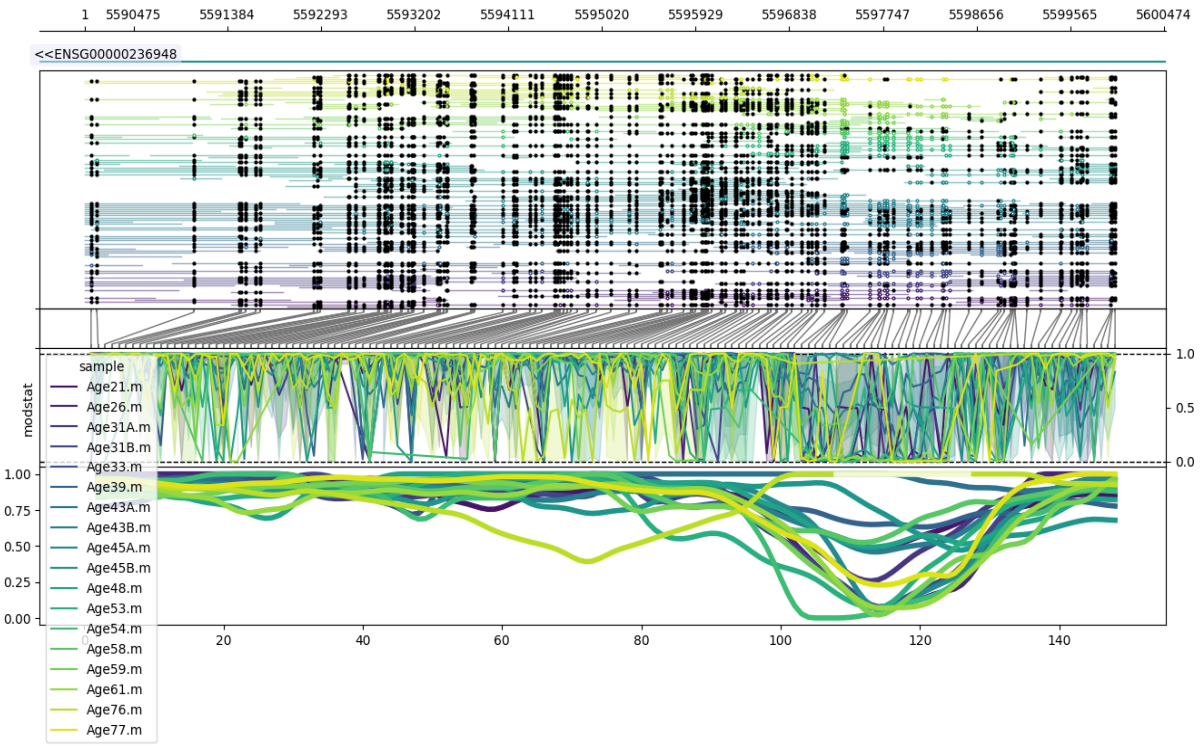

Figure 2. A closer view of the red circle region shown in Figure 1. When we examine the selected region more closely, the difference in methylation rate between samples is seen more clearly. Also, the dots in the upper part of the graph represent the methylations at that position and show that the darker the colour, the higher the methylation rate. As can be seen, the dark blue line represents the oldest sample, while the light yellow line represents the youngest sample. And in the differentiation area, the older samples had a high methylation rate, while the younger samples were grouped in the low methylation area.

Solar active region extraction using statistical methods

Martin Sanner[1], Dr. Karen Meyer[2], Prof. Stephen McKenna[3]

[1] University of Dundee, 2472597@dundee.ac.uk
[2] kmeyer001@dundee.ac.uk
[3] s.j.z.mckenna@dundee.ac.uk

Abstract

Solar active regions are areas on the surface of the Sun (Photosphere) where the magnetic field is particularly strong. Active regions are the main source of solar eruptions, which are sources of space weather events. As space weather is an important factor in running spacecraft, but also for electric systems on earth, understanding how eruptions form is vital to keeping protecting these systems. As such, understanding how solar active regions form and evolve is an important goal to achieve, which so far has been elusive because of the impact of the solar dynamo (and internal magnetic field structure) on active regions. To gain headway in this regard, we need to monitor active regions throughout their lifetime.

We have built a region detector using the statistics found from a synthetic dataset of active regions. To detect regions throughout their lifetime, first we attempt to find an active regions' first formation. The two main types of data we consider are magnetograms (direct measurements of the solar magnetic field from one perspective) and synoptic maps (combinations of magnetograms over time allowing one to estimate a full view of the solar surface over the month – e.g. (Figure 1), showing the prediction of our system for one synoptic map at Carrington Rotation 675 (1 Carrington Rotation = ~ 27.27 Days)).

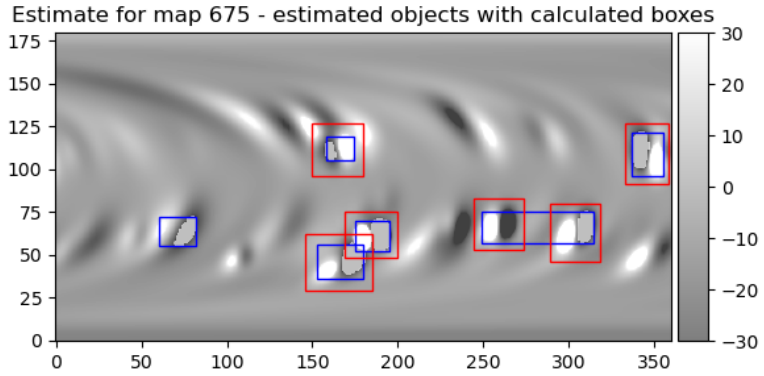

Figure 1: Synoptic Map for CR675, dataset active regions (ground truth) marked in a red bounding box, predicted regions marked in blue bounding boxes. White pixels show positive magnetic fields, black pixels negative fields.

Given a set of active region detections on some maps (synoptic or magnetograms), our pipeline estimates distributions for relevant parameters of the active regions, using those to sort pairs of connected components found in the image. Active regions can consist of multiple magnetic bipoles. Individual poles can be discovered with thresholding of the data, after which the distributions built up can be applied to estimate the likelihood of two poles forming a viable bipole. From these estimates, bipoles are formed and predicted as a newly forming active region if the magnetic field in that location has increased since the last measurement and the statistics of the region line up with expected values. For synoptic maps, this approach achieves an average precision of 0.93 (with a maximum possible average precision being 1, minimum 0). Next, this will be tested on observed synoptic maps, using datasets of active regions in observed maps for validation.

By design, this approach should be viable when employing magnetograms instead of synoptic maps. On achieving a similar average precision to synoptic maps on magnetograms, we aim to extend the system to track active regions throughout their lifetime from magnetogram measurements. Once this is complete, an approach to build lifetime statistics will be established.

POSTER PRESENTATIONS

(In order of programme)

University of Dundee

Simulating the effect of a Single Element Focused Ultrasound Transducer various distances from skull

Saeed Charbenny[1], Zhihong Huang[2], Tom Gilbertson[3]

[1] University of Dundee, 2403602@dundee.ac.uk

[2] z.y.huanf@dundee.ac.uk

[3] t.gilbertson@dundee.ac.uk

Abstract

An ultrasound transducer is a popular device for its non-invasive approach. The placement of the transducer relative to the skull can result in different outcomes. Investigating the various distance of a single element focused transducer from the skull with the aid of simulation can give an understanding on the different outcomes that are associated with focused ultrasound exposure.

The simulation is based on an experimental focused transducer and skull. The transducer was connected to an amplifier. The input signal was 70mV, amplified to 1W output with 666KHz. Hydrophone was placed at the focal point of 75mm. The pressure was recorded before and after the addition of the skull. The placement of the skull was 4mm away from the transducer to investigate the effect of skull addition. The design and information of a skull that was used for simulation were extracted from a CT scan. The scan was imported onto a 3D slicer with a minimum threshold of 300. The design of the skull with the addition of a transducer was made with Solidworks. The final design was imported onto Onscale, where the simulation was conducted.

The resulting pressure and intensity, of the focal point all remained within similar range as the skull was moved away from transducer. The effect of adding a skull was a pressure loss ranging from 84 to 88% compared to no skull. Another observed factor is the effect of different skull anatomy. Heterogenous skulls caused less effect on focal point change compared to homogenous. The effect of heterogenous ranged between 3 to 5 mm difference from the original focal point. On the other hand, a homogenous skull in the range of 10 mm difference from original. In addition, the further the skull, the closer the focal point to its original place vertically. Simulation aided in pointing out the effect of cancellous (trabecular) bone area, which in the experimental case, is filled with water which is the reason for lower focal point change compared to homogenous being mostly compact. The skull pressure remained in similar range close to transducer while increased as the skull is reaching the focal point as can be seen in figure 1.

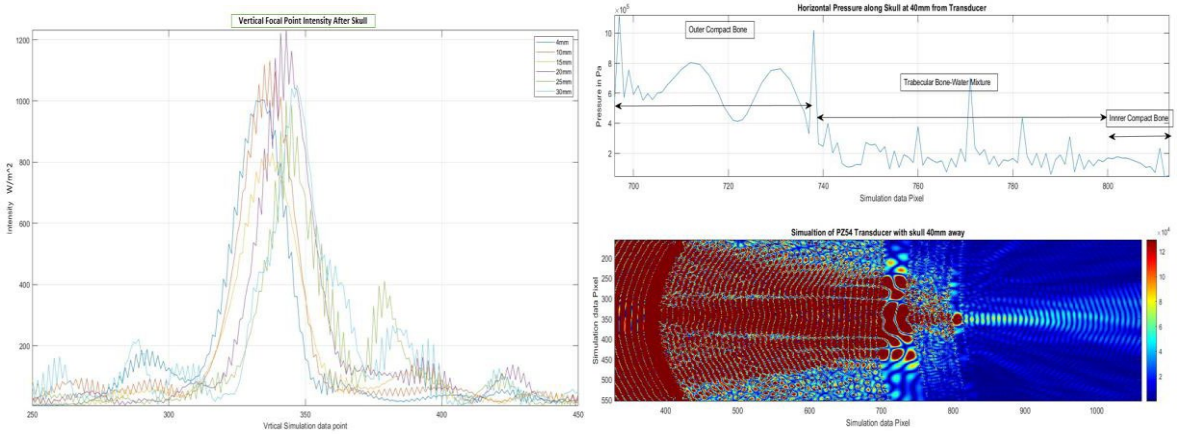

Figure 1: Vertical intensity on the focal point and pressure inside the skull

University of Dundee

Can consumer desktop additive manufacturing produce reproducible microscale feature parts?

Andrew Dennison[1], Nikola Krstajic[2], Ghulam Nabi[3]

[1] School of Science and Engineering, University of Dundee, 014009242@dundee.ac.uk,

[2] n.krstajic@dundee.ac.uk

[3] School of Medicine, University of Dundee, g.nabi@dundee.ac.uk

Abstract

Can consumer desktop additive manufacturing (AM) offer reproducible microscale (range 10-100µm) feature parts? Or is this only achievable using expensive industrial AM systems with advanced infrastructure? The rationale of this research was to validate if desktop AM was suitable for biomedical applications at a feature scale required for micro-optic housing, micro-fluidics and endomicroscopy tip design.

Over the last four decades, AM technologies have grown from research curiosities originating in the mid-1980s, to 'rapid prototyping' industrial systems developed throughout the 1990s, to consumer '3D printing' systems through the 2010s. According to ISO52900:2021 [1], there are seven recognized AM process categories: binder jetting (BJT), direct energy deposition (DED), material extrusion (MEX), material jetting (MJT), powder bed fusion (PBF), sheet lamination (SHL) and vat photopolymerization (VPP). These AM technologies allow the processing of solid, powder or liquid stock materials, ranging from thermoplastics and plastic polymers to metals, ceramics, composites and bio-materials. The common layer-by-layer approach of AM allows for the fabrication of parts and assemblies with geometries that would be physically or economically unsuitable for subtractive machining and formative manufacturing workflows. With the expiration of original patents in MEX and VPP, the last decade has seen substantial growth in companies developing consumer (<£1k) and prosumer (<£10k) desktop AM.

In this work, the objective was to develop a calibration workflow with test artefacts and implement using a benchmark reference desktop VPP system (Sonic Mini 8K, Phrozen) and selected photopolymer test resins; Aqua Gray 8K (Phrozen), Poliglass (Photocentric), Crystal Clear (Photocentric). This reference system fits the criteria of consumer desktop AM (<£1k) and uses a bottom-up UV light source (405nm, 1.725mW/cm^2) with an 8K (7500*3240) 22µm pixel liquid crystal display (LCD) mask for bitmapped image projection. A single moving (*z-axis*) translates a build-plate inside the liquid photopolymer vat to enable UV exposure patterns, with polymerization forming successive solid layers and an upside-down part. Priority was given to the direction of the transmitted light (*z-axis*) for calibration of exposure time (E_x) against cure depth (C_d). Tolerance optimization was used for the calibration of *x and y-axis* features.

Test artefacts reviewed in ISO52902:2019 [2] focus on *x and y-axis* aligned features >100µm. Some artefacts were scaled down to target 10µm minimal features, but new test artefacts were designed to target the priority z-axis calibration. Test AM was conducted with a range of exposure times (0-20s). Optical measurement was conducted using a trinocular microscope (SM-4TZ-3PL, AMSCOPE) fitted with a 24MP camera (α ZV-E10, Sony), and all images globally calibrated with a USAF-1951 test target in ImageJ software (NIH, USA). A minimum measurement sample of (n=15) was used for each exposure time to provide statistical metrics. A 'Jacobs Working Curve' [3] approach was used to graph exposure energy (mW/cm2) vs measured cure depth (µm). This allowed the extraction of key resin parameters, critical exposure energy (Ec) and penetration depth (Dp), used to calculate optimal exposure times. The calibration process was successfully verified by measuring test artefacts manufactured at the calculated optimal exposure time.

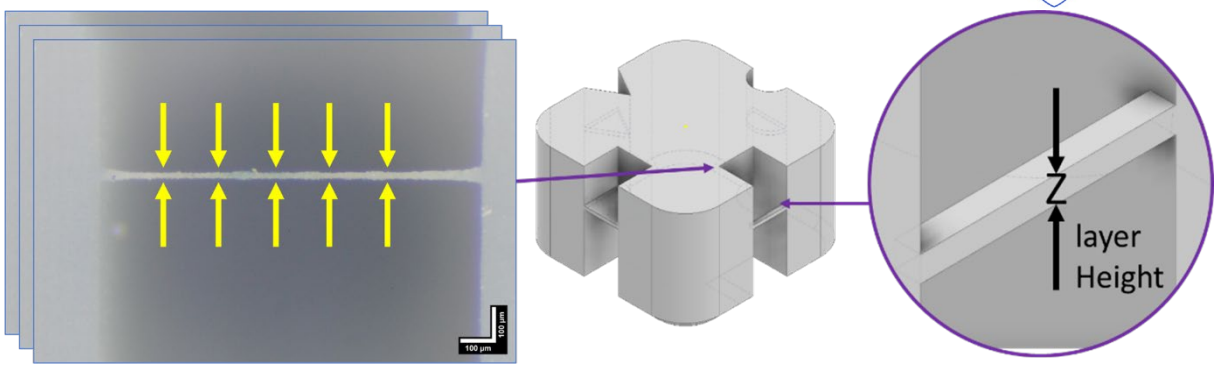

Figure 1: Calibration test structure schematic for (*z-axis*). Left insert, microscopy example images.

References

ISO/ASTM 52900:2021, Additive manufacturing - General principles - Fundamentals and vocabulary. Geneva, Switzerland: International Organization for Standardization (ISO); 2021.

BS EN ISO/ASTM 52902:2019 Additive manufacturing - Test artifacts - Geometric capability assessment of additive manufacturing systems. BSI Standards Publication, 2019.

P. F. Jacobs, "Fundamental Processes," in *Rapid Prototyping & Manufacturing Fundamentals of StereoLithography*, Society of Manufacturing Engineers, 1992, pp. 87–91.

Investigating the limitations of endomicroscopy and how they can be improved

Matthew Eadie[1], Nikola Krstajic[2], Jinpeng Liao[3], Ghulam Nabi[4], Wael Ageeli[5],

[1] Biomedical Engineering, University of Dundee, m.eadie@dundee.ac.uk

[2] n.krstajic@dundee.ac.uk

[3] j.y.liao@dundee.ac.uk

[3] Centre for Medical Engineering and Technology, University of Dundee, g.nabi@dundee.ac.uk

[4] Diagnostic Radiology Department, Jazan University, wageeli@jazanu.edu.sa

Abstract

Fiber-bundle endomicroscopy has several recognized drawbacks, the most prominent being the honeycomb effect. Fiber bundle endoscopes use many fibers (cores), between 5000 and 30,000, which act as sensors. The total size of the fiber bundle is usually <5mm in diameter; each core is then surrounded by cladding, which prevents light from affecting the surrounding cores. Due to the spacing and the cladding around each fiber, gaps are present between the cores that need to be filled to see a full image of the tissue. These gaps are normally filled using Gaussian blurring or linear interpolation. We developed a multi-frame super-resolution algorithm exploiting bundle rotation to extract features and reconstruct underlying tissue (Figure 1). Simulated data was used with rotated fiber-bundle masks to create multi-frame stacks to train the model. Super-resolved images are numerically analysed, which demonstrates that the algorithm can restore images with high quality. The mean structural similarity index measurement (SSIM) improved by a factor of 1.97 compared with linear interpolation. The model was trained using images taken from a single prostate slide, 1343 images were used for training, 336 for validation, and 420 for testing. The model had no prior information about the test images, adding to the robustness of the system. Image reconstruction was completed in 0.03s for images of size 256 × 256 pixels, indicating future real-time performance is within reach. The combination of fiber bundle rotation and multi-frame image enhancement through machine learning has not been utilized before in an experimental setting but could provide a much-needed improvement to image resolution in practice.

Image reconstruction methods can be a computationally costly processes that, if left unoptimized, require a large amount of time to complete. Machine learning introduced us to the benefits of GPU enhanced processing. By utilising techniques such as vectorisation alongside GPU processing, we are aiming to improve the processing time significantly and allow for real time image display (10+ fps). These methods will then be published and offered as an open-source library so that others may use our code on their own image or to further develop into their own fast processing methods. This work is currently still in progress, however, is showing significant progress by accelerating some functions by up to 10x.

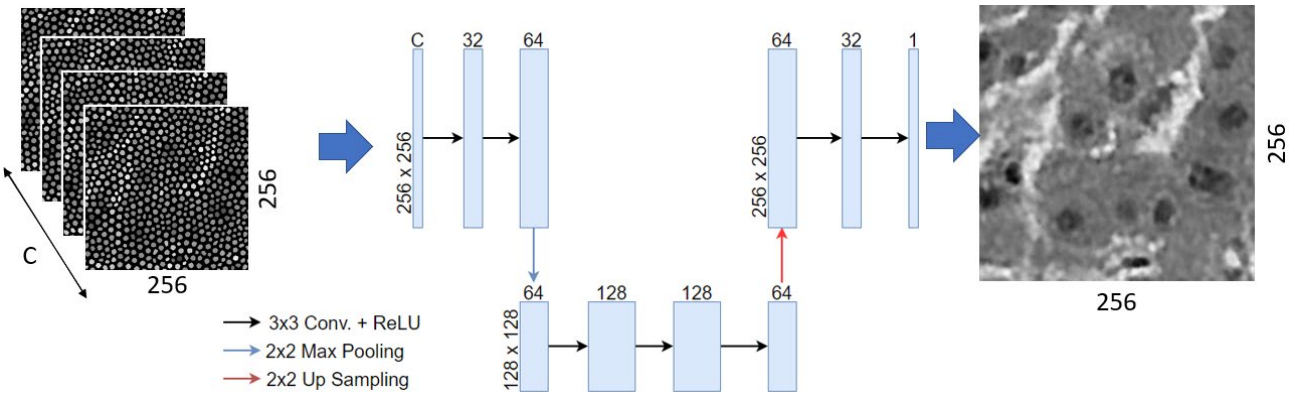

Figure 1 Proposed MFAE model. C represents the number of segments (channels) to be combined.

References

Eadie, M.; Liao, J.; Ageeli, W.; Nabi, G.; Krstajić, N. Fiber Bundle Image Reconstruction Using Convolutional Neural Networks and Bundle Rotation in Endomicroscopy. *Sensors* **2023**, *23*, 2469. https://doi.org/10.3390/s23052469.

A Deep Neural Network-based Method for Assessment of Wound Healing in Mice

Jinpeng Liao[1], Zhihong Huang[2], Chunhui Li[3]

[1] University of Dundee, jyliao@dundee.ac.uk

[2] z.y.huang@dundee.ac.uk

[3] c.li@dundee.ac.uk

Abstract

Different wound dressings should be applied depending on the stages of healing. Hence, it is crucial to understand the process of cutaneous wound healing in order to provide effective treatment. Current diagnosis methods, such as biopsy and dermoscopy, are highly invasive, contact, and lack depth information under the epidermis. In this study, acute wounds were introduced to mice and were imaged on Days 3, 5, 7, 10, and 14 with optical coherence tomography angiography (OCTA). The OCTA is a non-invasive imaging methodology that can extract moving blood flow signals from the relative static tissue, and provide depth information with ~2 mm and high-resolution with ~10 µm. Based on the different wound stages of OCTA images, this study aimed to apply a deep neural network (DNN)-based method to automatically classify the different wound healing stages. DNN can be separated into two main types: convolution neural network (CNN) and transformer (attention mechanism-based). Therefore, a competition study among a series of DNNs is further implemented to investigate the most suitable neural network for this study.

A swept-source (SS)-OCT system with an A-scan rate of 200 kHz was used to acquire data on wound healing stages in mice. After processing by the windowed eigen decomposition (wED)-OCTA algorithm [1] and enface projection algorithm, a total of 2750 enface images were extracted from the data, as shown in Figure 1. A series of data argumentation methods (e.g., horizontal flip, rotation, and normalization) were applied to those enface images to enhance the robustness of the trained network. Regarding the competitive results of the selected network, in Figure 2, seven types of neural networks were used in this study. As indicated in Figure 2 (A) and (B), among them, the DenseNet-121 [2] has achieved the highest accuracy (94%) in classifying the mice wound healing stages, while the network size is moderated (18m parameter) and smaller than ResNet-50 (25.6m parameter with 87% accuracy). The transformer-type networks (i.e., CCT (69%), ViT-large (50%), and CvT-21(84%)) have a worse competitive result than CNN-type, we hypothesis that is because of the limited amount of the data, while the training of the transformer network requires ~200k images [3].

Based on the competitive results, the DenseNet-121 is selected for the assessment of wound healing in mice, and the experiment results show that neural networks have the capability as an assistive method to classify the wound healing stages. In the future, we aim to collect the different healing stages of skin in the clinical environment and deploy the trained neural network to facilitate the wound healing stages recognition.

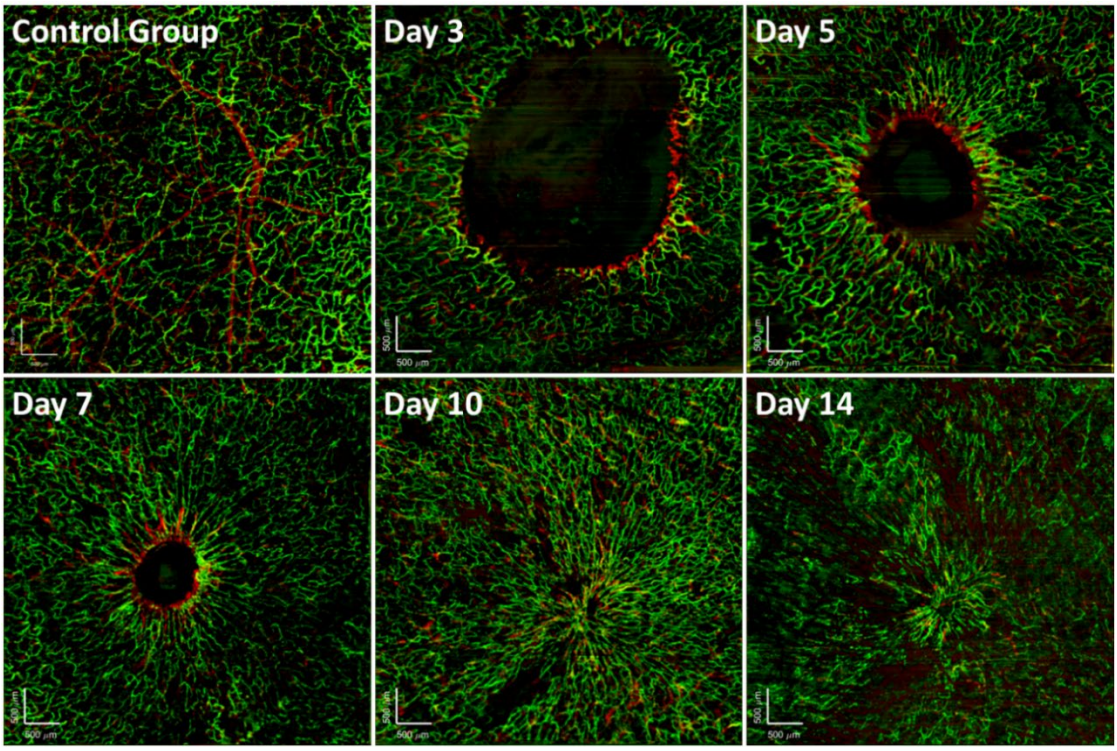

Figure 1. Different stages (days 'Control', 3, 5, 7, 10, and 14) of wound healing in a single mice. Imaging depth is between 0 mm and 1.27 mm, and maximum intensity projection method is used to acquire enface images per 85 µm. (All animal procedures were conducted with approval from the local ethical review committee at the University of Edinburgh and under regulations in 'Guidance on the Operation of Animals, Scientific Procedures act, 1986')

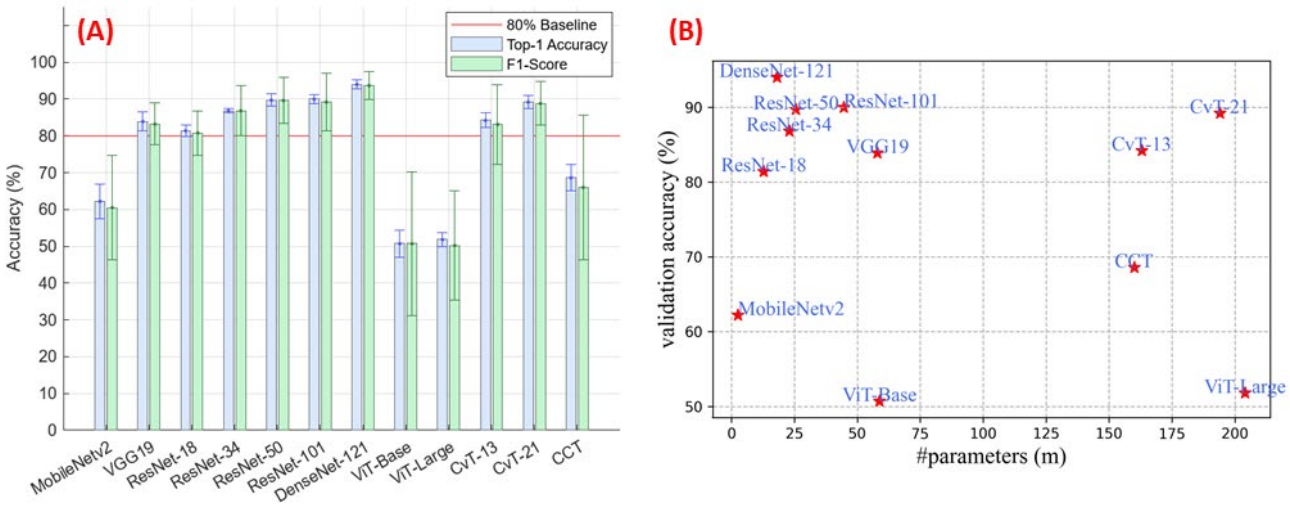

Figure 2 (A) Comparison of the wound healing stages classification accuracy between the different neural networks. (demonstrates in mean ± standard deviation) (B) Comparison between the neural network parameters (million) and classification accuracy. ViT: vision transformer; ResNet: residual neural network; CvT: convolutional transformer; CCT: compact convolutional transformer.

References

T. Zhang *et al.*, "Windowed Eigen-Decomposition Algorithm for Motion Artifact Reduction in Optical Coherence Tomography-Based Angiography," *Applied Sciences*, vol. 13, no. 1, p. 378, 2022.

G. Huang, Z. Liu, L. van der Maaten, and K. Q. Weinberger, "Densely connected convolutional networks," in *Proceedings of the IEEE conference on computer vision and pattern recognition*, 2017, pp. 4700–4708.

A. Dosovitskiy *et al.*, "An image is worth 16x16 words: Transformers for image recognition at scale," *arXiv preprint arXiv:2010.11929*, 2020.

University of Dundee

Photoacoustic Microscopy Imaging

Amirhossein Pourali[1], James Joseph[2], Ghulam Nabi[3]

[1] apourali@dundee.ac.uk

[2] jjoseph001@dundee.ac.uk

[3] g.nabi@dundee.ac.uk

Abstract

Photoacoustic imaging (PA imaging) is a revolutionary imaging technique used in medical applications since the late 1980s. Its origin can be traced back to Alexander Graham Bell's accidental 1880 observation that a chopped sunlight incident upon a solar cell produced an audible sound. The PA effect involves three energy conversions Field (Bell, 1881) (G. Diebold, 1991). The incident electromagnetic energy is first converted to thermal energy through rapid absorption by chromophores and then converted to mechanical energy through the thermoelastic effect. This creates a pressure wave that propagates away from the chromophores. To restore the incident optical power to an acoustic wave effectively, the laser pulse length must be shorter than two necessary time constants to satisfy thermal and stress confinement. This technique has created high-resolution images of biological tissue, allowing medical professionals to diagnose and treat medical conditions more accurately.

Photoacoustic (PA) imaging is a powerful imaging modality that can be broadly divided into two categories: photoacoustic microscopy (PAM) and photoacoustic tomography (PAT). PAM uses a focused laser beam to achieve high spatial resolution imaging at shallow depths. At the same time, PAT involves broader illumination schemes for deeper penetration, with the ultrasound transducer dictating spatial resolution. Both can be performed with optical or acoustic resolution configurations (al., 2014) (C. Zhang, 2010). In recent years, advances in light delivery technologies have led to the development of PA imaging systems that are more mobile, tuneable, compact, and affordable. Despite these advantages, PAM is still limited by sound speed, making it unsuitable for high-speed imaging processes. Furthermore, the technique has other limitations, such as the inability to provide accurate images of specific structures or penetrate deep into large tissue samples. Therefore, further research and development are needed to enhance the capabilities of PAM and make it a more versatile imaging modality (S. Park, 2014).

This project aims to improve the performance of photoacoustic microscopy imaging by optimising the laser light source and signal processing algorithms and by implementing advanced imaging techniques such as dual-wavelength imaging, multi-mode imaging and high-speed imaging. Additionally, several methods can be employed to improve further the resolution, imaging depth, signal-to-noise ratio, and speed of photoacoustic microscopy. These include the implementation of higher-frequency transducers and higher pulse energies and using diffractive optical elements, noise-reduction algorithms, a faster laser pulse repetition rate, an optimised scanning algorithm, and a faster transducer with higher bandwidth. A nonlinear detection algorithm, such as compressive sensing, and a light-scattering medium, such as an optical clearing agent, can further enhance the imaging process. By combining these different techniques, photoacoustic microscopy can be made even more efficient and effective. This will allow for reduced imaging time, increased resolution, and improved imaging speed, thus providing more comprehensive insight into biological systems and enabling more accurate diagnosis and treatment.

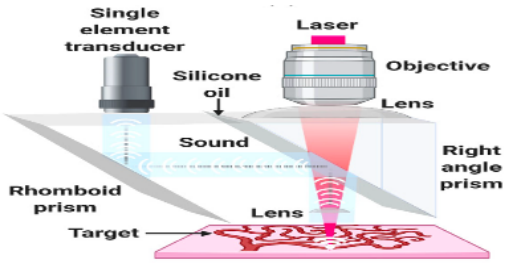

Figure 1 Typical PAM setup (Pramanik, 2017)

References

sub-wavelengthal., W. S. (2014). Reflection-mode in vivo photoacoustic microscopy with sub- wavelength lateral resolution. *Biomed. Opt. Express , 5*(12), 4235–4241.

Bell, A. G. (1881). LXVIII. Upon the production of sound by radiant energy. *Lond. Edinb. Dublin Philos. Mag. J. Sci, 11*(71), 510–528.

C. Zhang, K. M. (2010). Subwavelength-resolution label-free photoacoustic microscopy of optical absorption in vivo. *Opt. Lett, 35*(19), 3195–3197 .

G. Diebold, T. S. (1991). Photoacoustic monopole radiation in one, two, and three dimensions. *Phys. Rev. Lett., 67*(24), 3384–3387.

Pramanik, M. M. (2017). Performance characterization of a switchable acoustic resolution and optical resolution photoacoustic microscopy system. *Sensors, 17*(2), 357.

S. Park, C. L. (2014). Acoustic resolution photoacoustic microscopy. *4*(3), 213–222.

The Importance of Microfabrication in Healthcare: Enabling Personalized and Complex Medical Devices

Daiyuan Xie[1], Nikola Krstajic[2], Chunhui Li[3]

[1] 2532030@dundee.ac.uk

[2] n.krstajic@dundee.ac.uk

[3] c.li@dundee.ac.uk

Abstract

Micro-manufacturing has become increasingly important in healthcare as it enables the production of complex and precise medical devices and implants tailored to individual patient needs. Micro-manufacturing holds great promise with the advent of 3D printing, which enables the production of intricate geometries with exceptional precision and accuracy. In this context, the photo-polymerisation reaction is a widely used process for 3D printing, as it allows the fabrication of structures with high resolution and resolution.

The photopolymerization process involves using a light source to trigger a chemical reaction that converts a liquid resin into a solid polymer. The resin contains photo initiators, which absorb light energy and generate free radicals that initiate the polymerisation reaction. The reaction proceeds layer-by-layer fashion, each layer cured by the light source before the next layer is added. With this capability, intricate three-dimensional structures can be fabricated with exceptional precision and accuracy.

To ensure the accuracy and quality of the 3D printing process, simulation software such as COMSOL is often used. COMSOL is a multiphysics simulation software that allows the modelling of physical phenomena such as fluid dynamics, heat transfer, and chemical reactions. In the context of 3D printing, COMSOL can be used to simulate the photo-polymerisation process and predict the properties of the printed structures, such as mechanical strength, porosity, and surface roughness.

The simulation principles of COMSOL involve the creation of a mathematical model that describes the physical phenomena of interest. Upon applying numerical techniques to solve the model, the resultant outcomes are examined and illustrated through visualization and analysis. COMSOL allows the creation of complex models with multiple physics and geometry domains, providing a user-friendly interface for setting up and solving the models.

The importance of microfabrication in the biomedical field lies in its ability to produce medical devices and implants with high precision and accuracy, which can improve patient outcomes and reduce healthcare costs. Advanced microfabrication techniques like 3D printing can facilitate the production of intricate structures that are challenging or unfeasible to manufacture using conventional methods. Additionally, microfabrication can allow the production of personalised medical devices and implants tailored to individual patient needs, improving patient comfort and quality of life.

In conclusion, micro-manufacturing using 3D printing and the photo-polymerisation reaction has excellent potential in healthcare. Simulation software such as COMSOL can ensure the accuracy and quality of the 3D printing process, and microfabrication techniques can enable the production of complex and personalised medical devices and implants. The importance of microfabrication in the biomedical field lies in its ability to improve patient outcomes and reduce healthcare costs. The possibility of assuming a progressively essential position in the healthcare industry is likely for it in the future.

Electrical impedance of an ultrasonic needle device as an indicator of needle tip position

Youheng Zeng[1], Zhihong Huang[2], Graeme McLeod[3]

[1] University of Dundee, 170023294@dundee.ac.uk

[2] z.y.huang@dundee.ac.uk

[2] Consultant Anaesthetist, Institute of Academic Anaesthesia, Ninewells Hospital, NHS Tayside, g.a.mcleod@dundee.ac.uk

Abstract

Purpose: Ultrasound-guided percutaneous needle procedures are commonly conducted in regional anaesthesia and tissue biopsy in clinics. However, accurate needle tip localisation remains a challenge. Insertion force is practically used as a biomarker of the needle tip position. In this study, with reference to insertion force, we explore the potential of using the real-time electrical impedance of an ultrasonic needle as an indicator of needle tip location.

Methods: The ultrasonic needle device (Fig. 1a) employed a piezoelectric Langevin ultrasound transducer to longitudinally actuate a common anaesthesia needle. The resonance mode of the ultrasonic device was determined through numerical simulations and experimental validations, allowing it to maintain high vibration amplitudes while sensing mechanical loads on the needle. A control module was used to track the resonance frequency and stablise the vibration amplitude of the device, while providing real-time measurements of the electrical impedance of the device, which varies with the mechanical loading applied by the tissue during needle procedures. The insertion force acquired from a force sensor was also monitored during needle insertions.

Gelatin phantoms with concentrations of 10%,15% and 20% were used for single-/multi-layer testing objects. A skin-mimicking layer made of silicone was used in multilayer phantoms to introduce puncturing during needle insertions. For single-layer phantom experiments, the needle was inserted at 1 mm/s until it reached the targeted depths of 5, 15 and 25mm, where the device was then kept stationary. For multi-layer phantom experiments, the needle was inserted at 1mm/s until all phantom layers were punctured.

Results: Higher impedance magnitudes were observed with greater insertion depths and stiffer phantoms (Fig. 1b), and this trend closely mirrored changes in insertion force. Both metrics proved effective for identifying key events during needle insertions, including puncturing and entering a new layer. While insertion force lacked utility when the needle was stationary, impedance magnitude reliably indicated insertion depth in homogeneous phantoms. Overall, the electrical impedance measured by our integrated system has a strong potential to be a useful feedback signal to improve percutaneous needle procedures.

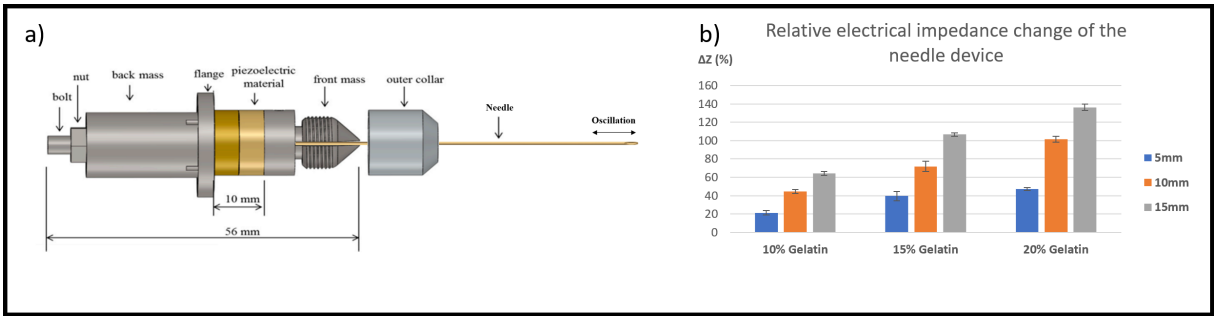

Figure 1: a) Ultrasound-actuated needle device b) Electrical impedance change of the needle device in percentage

Development of a Handheld Swept-Source Optical Coherence Tomography System with High-Speed Acquisition

Tianyu Zhang[1], Zhihong Huang[2], Chunhui Li[3]

[1] University of Dundee, txzhang@dundee.ac.uk

[2] z.y.huang@dundee.ac.uk

[3] c.li@dundee.ac.uk

Abstract

Optical Coherence Tomography (OCT) has become a developed and common imaging methodology for ophthalmology and dermatology. With ultrahigh A-scan rates, Swept-Source OCT (SS-OCT) technique is often favourable for the OCT Angiography (OCTA) function. Therefore, we developed a lab-built SS-OCT system, which is handheld, portable, non-invasive, high-resolution, and high-speed acquisition, with angiography and elastography (OCE) functions.

This system utilized a swept-source laser with a centre wavelength of 1300 nm, a sweeping range of 100 nm, and a 400 kHz sweep rate. Due to its high sweep rate, the system's maximum A-scan rate could reach up to 400 kHz, although the scanning depth was decreased to around 1.5 mm. After being generated from the laser source, the light beams would pass through a circulator and a 50/50 beam splitter which could split the light into the reference arm and the sample arm. On the reference arm, the polarization controller and the collimator could be rotated or moved by motors, which were connected to a customised PCB board. At the end of the reference arm, a lens and a mirror were installed to match the optical length of the sample arm. On the sample arm, i.e., the scanning probe, a set of galvo mirrors was used to control scanning directions. In addition, an LSM03 lens, a dichroic mirror and a CCD camera were also integrated inside the probe. With a display screen, the scanning probe could be easily used for handheld acquisitions. After the interference between the two arms, a balanced photodetector and a PCI-e digitizer could receive signals with a high sampling rate. Lastly, the operation software required LabView and MATLAB, while post-processing could be achieved with MATLAB or Python.

This poster will present a non-invasive handheld SS-OCT system with an ultrahigh A-scan rate with a scanning range of around 15 mm on both axes, while its penetration depth is around 1.5 mm. The lateral resolution is 19.68 µm, and the axial resolution is 8.47 µm. In addition, by adjusting the scanning protocol, this system can achieve OCTA and OCE functions. Hence, this system can be used for wound healing monitoring, cancer diagnosis, and several other potential applications.

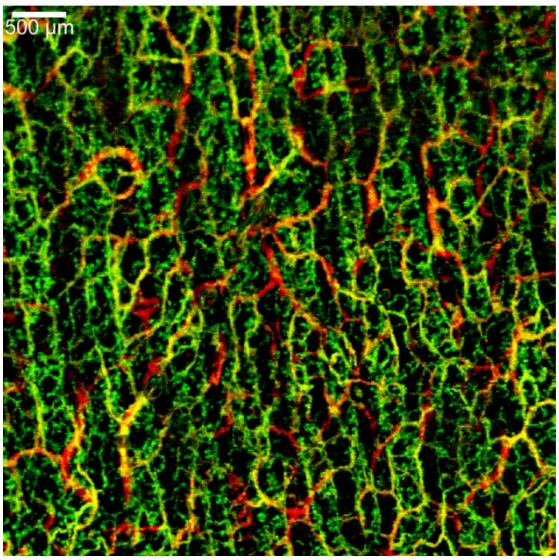

Figure 1: OCT Angiography imaging a finger tip.

Quantifying the impact of source variability on buoyant jet behaviour

Morgan Hetherington[1], Dr Alan Cuthbertson[2], Professor Sue Dawson[3], Dr Fabio Dioguardi[4]

[1] Civil Engineering, University of Dundee, 140010768@dundee.ac.uk

[2] a.j.s.cuthbertson@dundee.ac.uk

[3] Geography and Environmental Sciences, University of Dundee, s.dawson@dundee.ac.uk

[4] University of Bari, Dipartimento di Scienze della Terra e Geoambientali, Fabio.dioguardi@uniba.it

Abstract

Buoyant jets and plumes are generated as a result of both natural and industrial processes (e.g. volcanic eruptions, marine wastewater discharges, and industrial atmospheric emissions) that can exhibit significant deleterious social, economic and environmental impacts. For example, the 2010 eruption of Eyjafjallajökull in Iceland disrupted European and North American airspace for over a month, causing significant social disruption and costing the aviation industry billions of dollars. One month later, the deep-water horizon oil spill occurred near the Gulf of Mexico, resulting in the degradation of many coastal habitats and fisheries. It is therefore crucial to understand the physical behaviour of buoyant jets in order to predict and mitigate against their socio-economic and environmental impacts.

Buoyant jets are comprised of two flow regions: a momentum-driven jet region close to the source (near-field) and a buoyancy-driven plume region far from the source (far-field) (*see Figure 1*). Well-established theories have been developed to explain how source conditions in the jet region affect downstream plume behaviour and form the basis of numerical models that predict buoyant jet behaviour. However, due to practical limitations, it is difficult to measure quantitative data directly at the source. On this basis, time-averaged source conditions are often assumed in buoyant jet models, which in turn eliminates variability in downstream plume behaviour linked to source unsteadiness. Observations of field scale buoyant jets have revealed fluctuations in source conditions (e.g. pulsatory volcanic eruptions or diurnal fluctuations in wastewater outfall discharges), indicating a potential disconnect between well-established steady-state buoyant jet theories and reality. This study aims to address this apparent disconnect by evaluating the impact of source variability on downstream plume behaviour through a combination of scaled experiments and numerical modelling. Experimental work involved combining fresh water with fluorescent dye or particles to create a low density ($\rho 1$ = 1000 kg/m^3) effluent, pumped into a homogeneous salt water ambient volume with density $\rho 2$ = 1010 - 1030 kg/m^3, generating a buoyant jet (*Figure 1*). The source flow rate Q was varied to achieve either steady-state or unsteady source conditions, allowing a range of parametric buoyant jet conditions to be investigated. To analyse downstream plume behaviour (i.e. centreline concentration and velocity, plume geometry, etc.) in response to changing source conditions, a variety of image analysis methods were employed, including particle-image velocimetry (PIV), ultrasonic velocity profiling (UVP) and light-induced fluorescence (LIF).

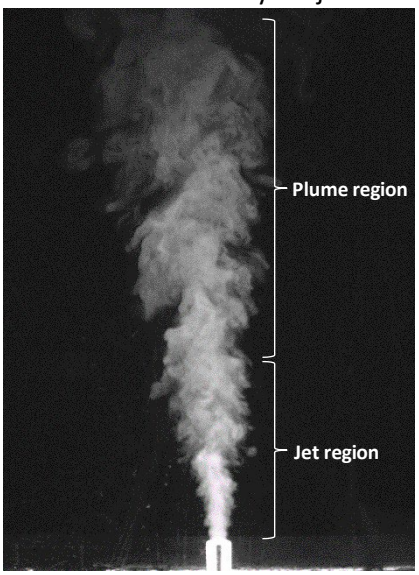

Figure 1. Dye image of a single-phase buoyant jet taken from experiments.

The numerical modelling aspect of this research aims to evaluate how well time-averaged plume models can replicate unsteady buoyant jet discharges, with the one-dimensional steady-state model FPLUME[1] used to simulate the highly unsteady 2010 Eyjafjallajökull eruption plume. Plume rise heights and mass eruption rates were predicted at 60 and 5-minute intervals during two explosive phases of the eruption, with results validated against observations taken from the C-band radar at Keflavik airport. Preliminary findings from experiments and numerical modelling will be presented, and their implications discussed.

References

Folch, A., Costa, A. & Macedonio, G. FPLUME-1.0: An integral volcanic plume model accounting for ash aggregation. *Geoscientific Model Development* 9, 431-450 (2016).

University of Dundee

Fluid-solid flow transitions in mixed (sand-mud) sediments: Enhanced modelling of sedimentation in estuarine and coastal waters

Yi Yuan[1], Alan Cuthbertson[2], Tom Eaves[3]

[1] University of Dundee, 2394028@dundee.ac.uk

[2] a.j.s.cuthbertson@dundee.ac.uk

[3] teaves001@dundee.ac.uk

Abstract

Sedimentation processes in natural estuarine or coastal sediment systems are normally divided into three regimes: (1) the *dilute settling regime*, where settling particles move independently, with minimal hydrodynamic interaction between each other; (2) the *hindered settling regime*, where volumetric concentrations of settling particles result in return flows and interactions generated by faster-settling particles affecting the settling rates of other slower settling particles; and (3) the *consolidation regime*, where the deposited bed layer is compressed by the overburden at the top of the settling unit due to gravity.

Figure 1 represents the structural evolution of a single-type (i.e. monodisperse) particle suspension, where the first two regimes (dilute and hindered settling) are represented by the 'Settling Zone', while the 'Gelled Zone' reflects the subsequent bed consolidation regime. The spatio-temporal transitions between these regimes are not currently well understood or modelled, particularly when considering the sedimentation behaviour of polydisperse mixtures of cohesive (i.e. mud) and non-cohesive (i.e. sand) sediments. The aim of the project will be to develop a new model for polydisperse hindered settling and multifractional, flow-driven compaction model, with experimental studies aimed at improving the physical representation of fluid-solid regime transitions for the cohesive and non-cohesive mixture during the sedimentation process.

The project has significant implications for improving predictions of mixed (i.e. sand-mud) sediment transport dynamics, as particularly crucial to maintaining navigation channels, ports and harbours, understanding morphological evolution in affected coastlines, and preserving and enhancing sensitive habitats (e.g. mudflats). The coupled numerical model development will be informed directly by laboratory experiments conducted in a bespoke settling column to study the physical settling and compacting characteristics, and solid-fluid regime transitions, for natural mixed sediments during sedimentation events.

Figure 2 presents preliminary model simulations of the evolving deposit height for a monodisperse suspension (i.e. cohesive clay particles only), comparing these predictions to experimental measurements for clay sedimentation. The accuracy of the model is largely controlled by several fitting parameters representing permeability, effective stress and the compacting rate for the monodisperse particles. The project will extend this model to include additional polydisperse interactions between cohesive and non-cohesive particles, taking account of processes such as aggregation and segregation in the resulting deposits.

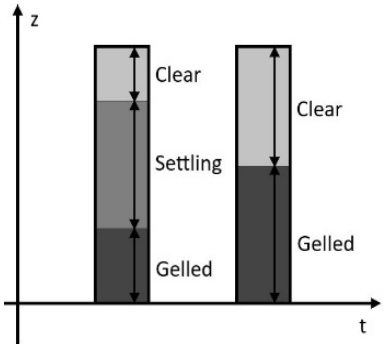

Figure 1 Geometry arrangements of polydisperse suspensions containing a single type of particles phase with time-lapses

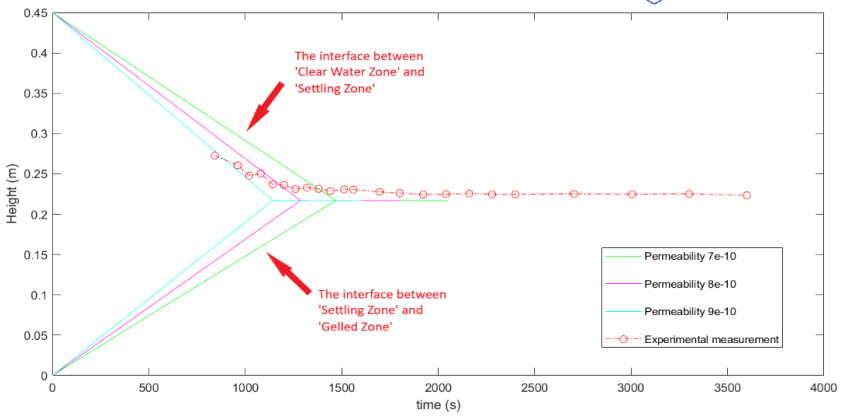

Figure 2 Model fitting line with varying parameters (permeability) setting of single-type particle polydisperse suspension

Development and evaluation of antibacterial surfaces for medical implants

Yimeng Wang[1], Qi Zhao[2], Svetlana Zolotovskaya[3]

[1] University of Dundee, yzzvwang@dundee.ac.uk

[2] q.zhao@dundee.ac.uk

[3] s.a.zolotovskaya@dundee.ac.uk

Abstract

Bacterial colonization and subsequent biofilm formation on surfaces of medical implants such as urinary catheters, ureteral stents or orthopaedic implants can lead to high infection rates of about 33% (Weinstein, R.A. and Darouiche, R.O. 2001), resulting in increased patients' morbidity and mortality. Many attempts have been made to prevent the implant associated infections by coating implants with antibiotics or silver. However, these coatings have the issues of either potential antimicrobial resistance or very limited anti-bacterial efficiency. Recently Prof Qi Zhao and his group developed a silver-PTFE nanocomposite coating with *optimum surface energy* that can effectively reduce bacterial adhesion and hence infection rate (Wang L & Zhao Q. et al. 2019). Nature-Inspired surfaces, such as lotus leaf and shark skin topographies, also exhibit excellent anti-bacterial properties (Arango-Santander, S., 2022). An advanced laser-based technique for production of micro/nano-structured surfaces have developed to replicate effects of natural antibacterial topographies. The aim of this PhD project is to develop biomimetic nano-textured surfaces with optimum surface energy prevent pin-site infections. As the pins for external bone fixation are made of medical titanium or stainless steel, a range of nano-textured surfaces have been designed and prepared on the two metallic substrates by a laser-induced nano structured technique under supervision of Dr Svetlana Zolotovskaya (see Fig 1a). To get optimum surface energy on the nano-structured surfaces, the nano-structured surfaces are coated with polydopamine-chitosan-silver nanoparticles (PDA-CS-AgNPs). The novel laser nano-structured surfaces with PDA-CS-AgNPs nanocomposite coating combine the non-stick properties of biomimetic nano-textured surfaces with optimum surface energy as well as the bactericidal properties of silver nanoparticles. Fig 1b shows that large number of bacteria adhered to the untreated titanium surface, and Fig 1c showed that a few bacteria attached to PDA-CS-AgNPs coated titanium surface. Clearly the coating possessed superior antibacterial activity. Future work includes: (1) to evaluate anti-bacterial efficiency of biomimetic laser nano-textured surfaces and find out optimum nanostructures; (2) to optimize the compositions of PDA, CS and AgNPs; (3) to apply the PDA-CS-AgNPs coatings to the nano-structured surfaces and to evaluate their anti-bacterial efficiency; (4) to use extended DLVO/steric interaction theories to gain insight into bacterial attachment mechanisms.

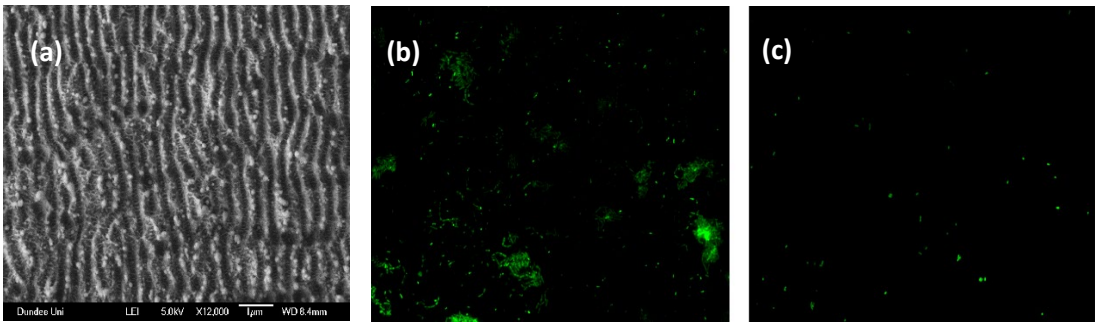

Fig 1 (a) nano-structured surface; (b) bacteria adhered to untreated surface; (c) bacteria adhered to coated surface

References:

Weinstein, R.A. and Darouiche, R.O. (2001). Device-associated infections: a macroproblem that starts with microadherence. *Clinical infectious diseases*, 33(9), pp.1567-1572.

Wang, L. & Zhao, Q et al (2019) In-vitro antibacterial and anti-encrustation performance of silver-polytetrafluoroethylene nanocomposite coated urinary catheters, *Journal of Hospital Infection*, 103(1):56-63

Arango-Santander, S. (2022). Bioinspired topographic surface modification of biomaterials. *Materials*, 15(7):2383.

Next Generation of RF Sensors for Digital Health Applications

Haoxuan Li[1], Wenda Li[2]

[1] Department of Biomedical Engineering, University of Dundee, 2525586@dundee.ac.uk
[2] wli001@dundee.ac.uk

Abstract

Digital health is a rapidly expanding field that utilises technology to improve healthcare delivery and outcomes. This includes the implementation of mobile health applications, wearable devices, telemedicine, and electronic health records. One of the key advantages of digital health is its ability to provide remote monitoring and care, which can enhance access to healthcare for individuals who are geographically or economically disadvantaged. Digital health offers vast potential for improving health and healthcare delivery by enhancing effectiveness, efficiency, accessibility, safety, and personalisation on a large scale. To achieve these advancements, it is crucial to develop novel hardware and algorithms to guide the development and implementation of digital health (Murray et al., 2016).

Passive Wi-Fi radar (PWR) is considered as a cost-effective, reliable, and non-invasive sensing technology. PWR employs existing Wi-Fi signals to detect and track moving objects such as vehicles, aircraft, or pedestrians. Unlike traditional radar systems, PWR detects radio waves emitted by Wi-Fi access points and routers rather than emitting radio waves and detecting reflections (Li et al., 2020). Especially, PWR measures the Doppler shift in the reflected Wi-Fi signal to calculate the object's velocity and direction and the time delay to calculate the object's range from the Wi-Fi transmitter.

PWR provides several useful outputs, including the Doppler shift that supplies information about the object's velocity and direction and range that offers the object’s distance from the Wi-Fi transmitter. By combining these outputs, passive Wi-Fi radar can accurately estimate the object's position.

PWR holds potential applications in remote patient monitoring in digital health. It could be used to monitor patients' movements and identify falls or abnormal behaviour (Li et al., 2022). This could lead to a more efficient and accurate way of monitoring and tracking patients, reducing the need for in-person visits and improving access to healthcare. However, using Wi-Fi signals for surveillance raises privacy concerns that must be carefully considered.

Commercial off-the-shelf (COTS) equipment will serve as the front end of radio frequency (RF) in this project. The USPR-2920 is selected to prototype and deploy wireless systems with custom signal processing. The above components will be prototyped with LabView to verify their feasibility and ability to demonstrate in real-time. This prototype will function like an RF sensor.

The WiFi hardware control and protocol adaption will be accomplished using C/C++. They will be utilised to extract WiFi radar information, including phase, frequency shift, and movement, with the network interference card. A computer will process signals, including cross ambiguity function, direct signal cancellation, and time-frequency analysis with MATLAB, like Figure 1.

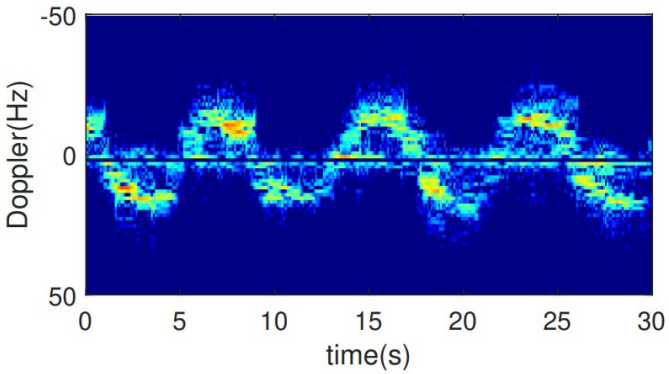

Figure 1: Doppler spectrogram of a single person walking.

References

Li, W., Bocus, M.J., Tang, C., Piechocki, R.J., Woodbridge, K. and Chetty, K. (2022). On CSI and Passive Wi-Fi Radar for Opportunistic Physical Activity Recognition. *IEEE Transactions on Wireless Communications,* 21(1): 607–620.

Li, W., Piechocki, R.J., Woodbridge, K., Tang, C. and Chetty, K. (2020). Passive WiFi Radar for Human Sensing Using a Stand-Alone Access Point. *IEEE Transactions on Geoscience and Remote Sensing,* 59(3): 1–13.

Murray, E., Hekler, E.B., Andersson, G., Collins, L.M., Doherty, A., Hollis, C., Rivera, D.E., West, R. and Wyatt, J.C. (2016). Evaluating digital health interventions: key questions and approaches. *American journal of preventive medicine,* 51(5): 843–851.

Handheld probe design for internal cancer in Optical Coherence tomography based on Elastography

Zhengshuyi Feng[1], Zhihong Huang[2], Chunhui Li[3]

[1] University of Dundee, 180021128@dundee.ac.uk
[2] z.y.huang@dundee.ac.uk
[3] c.li@dundee.ac.uk

Abstract

Early cancer detection plays an essential part in the prompt treatment of cancer. In addition to allowing doctors to analyse the disease and provide timely assistance to patients, this will also reduce the mortality rate of cancer and reduce patient suffering due to early treatment. Cancerous lesions lead to alterations in the mechanical properties of the cancerous tissue, particularly in stiffness, which can be stiffer than healthy tissue (Li et al., 2012). By evaluating the Young's modulus of the tissue the state of the lesion can be determined. Optical Coherence Tomography (OCT) is a potential candidate to meet this requirement, as the micron-level resolution of the OCT system allows for the detection of early cancerous tissue. And Optical Coherence Tomography based on Elastography (OCE) could combine with a stimulate device to investigate the elasticity of the sample. For internal cancers, such as rectal cancer prostate cancer and cervical cancer, an endoscopic probe was required to be designed to reach into the organ for detection. However, the size of the sample arm in the current design of the OCT system limits its ability to detect internal organs, also, the sample arm is currently fixed and cannot be movable.

This study describes a handheld OCT probe that takes advantage of the small size of the micro-electro-mechanical systems (MEMS) mirror which could replace the galvo-mirror system to achieve a movable and smaller sample arm. Meanwhile, the air-puff nozzle would be designed as a stimulation system inside the OCT probe. Due to the MEMS mirror serves the same purpose as the galvo-mirror system, so that the MEMS mirror can be designed in the endoscope as a scanning engine for the OCT probe. Furthermore, the air-puff system has the advantage of being contactless, easy-control and non-invasive, which can be used as an excitation device to provide airflow to the sample. The air-puff system generates short duration pulse with a wide bandwidth of surface waves to stimulate the sample being measured. In the sample arm of the OCT system, the laser can be focused through the lens and then reflected by the MEMS mirror onto the sample. The MEMS mirror allows for dual-axis scanning and is expected to enable 3D imaging of OCT systems in the future. For future improvements in design, MEMS mirror will be improved to smaller sizes, enabling internal cancer detection with smaller probe sizes. The design diagram of the OCT probe in SolidWorks is shown in Figure 1 as following.

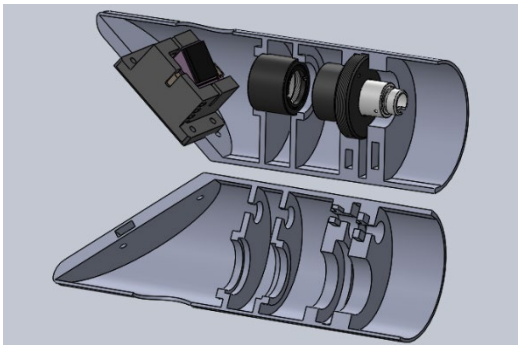

Figure 1: Diagram of OCT probe design

References

Li, C., Guan, G., Reif, R., Huang, Z., Wang, R.K., (2012). Determining elastic properties of skin by measuring surface waves from an impulse mechanical stimulus using phase-sensitive optical coherence tomography. *J. R. Soc. Interface*. (9), 831–84

University of Dundee

Cortical and trabecular bone ageing in the elderly: a 2D-3D approach on the rib and metatarsal

Jeffrey Daniel Anderson[1], Julieta Gomez Garcia-Donas[2], Craig Cunningham[3]

[1]Center for Anatomy and Human Identification, University of Dundee, 2517253@dundee.ac.uk

[2]jgomezgarciadonas001@dundee.ac.uk

[3]c.a.cunningham@dundee.ac.uk

Abstract

Bone is a highly organised composite material comprised of organic and mineral components, coming together to form the two macroscopic types of bone, cortical and trabecular bone. Cortical bone is the dense outer layer, has very low porosity, low metabolism and predominantly supports loading; trabecular bone comprises web-like interconnected plates and rods and, conversely, is highly metabolic, highly porous, and redistributes loads to cortical bone.

Ageing affects bone repair (remodelling) in both sexes, generally starting earlier in women due to decreased oestrogen production in menopause, creating a negative balance of old bone being removed and newly bone being formed. Microscopic changes are initially seen in the trabecular bone due to its high surface area and high metabolic activity, but later become more significant in the cortical bone.

Notable microscopic age-related cortical bone changes include increased osteon number, changes in osteon size and shape, decreased relative area, and increased porosity. Trabecular bone age-related changes include decreased number and connectivity of struts, increased spacing between trabeculae, change in shape from plate-like to rod-like, and decreased directionality of trabeculae (anisotropy). In general, these trabecular changes result in reduced redistribution capacity, while the cortical thinning and increased porosity reduce ability to provide primary support. The present research aims to investigate age- and sex-related patterns related to microscopic changes in cortical and trabecular bone in an elderly Scottish population through comparison of 2D microscopy (histomorphometry) and 3D micro-computed tomography (microCT).

The samples will include the left 6th rib and 5th metatarsal from Thiel embalmed (soft-fixed) elderly donors from the University of Dundee. Ribs are relatively well-studied skeletal elements in bone histomorphometry. The metatarsals, however, are novel bones for use in bone histology or aging in clinical and forensic research, considered herein as they are easy to extract and generally well protected in forensic cases when enclosed in footwear. Moreover, the 5thmetatarsal, specifically, has relatively low loading amongst the bones of nonpathological feet. The cortical and trabecular data will be analysed exploring the correlation of the parameters with age, and further comparisons will be performed investigating age-related changes between the sexes and age cohorts.

The findings from this study are expected to provide a better understanding on how aging impacts bone mechanical and material properties in the elderly, offering further insight with clinical implications in relation to fracture risk and age-related pathological conditions such as osteoporosis. Additionally, findings may provide further strength and evidence to the field of forensics and ageing if predictable age-related patterns are detectable.

Developing the standards used in facial approximation: a geometric morphometric investigation of the eye across three populations: European, Arab, and South Korean

Kailey Lohmann[1], Dr. Tobias Houlton[2], Prof Fordyce A. Davidson[3]

[1] Centre for Anatomy and Human Identification, klohmann@dundee.ac.uk
[2] thoulton001@dundee.ac.uk
[3] fadavidson@dundee.ac.uk

Abstract

In forensics, facial approximation refers to the process of estimating the face from a skull to support unidentified person inquiries. It is used as a last resort when more objective methods of identification (DNA, finger printing, dental records, radiographic records) have failed or are not available. The generated facial depiction is intended to promote recognition, and in turn facilitate new investigatory leads. Facial approximation is often criticised for being highly subjective, with existing protocols often demonstrating small sample sizes, contradictory guidelines, and sometimes being based on informal observations that lack empirical evidence to support their application. Despite these limitations, the field has enabled successful recognition and demonstrated real-world value – hence its continued application today.

To enhance existing standards in facial approximation, geometric morphometric techniques are being utilized to study and develop new and robust prediction protocols from spatial trends in craniofacial coordinates relevant to the eye region – a critical feature relevant to face perception and recognition. This is an ongoing investigation that will eventually incorporate 237 clinical scans (CT and MRI) of individuals aged between 20 and 70 years, comprising population groups from Yemen, South Korea, and Europe. The clinical images will be viewed and anterior 2D images of the skull and face set in the Frankfort Horizontal Plane captured using DICOM viewer, OsiriX. Predetermined hard and soft tissue landmarks will be plotted on these images using TPSDIG2, a geometric plotting software. Geometric morphometric tests will then be performed using MorphoJ. To test for inter- and intra-observer repeatability when identifying and plotting landmarks, the Procrustes distance will determine the measurement error. The mean vector of each cephalometric landmark that corresponds to a homologous craniometric landmark location will then be determined. A Principal Component Analysis and Canonical Variate Analysis will be used to establish patterns in eye morphology. A two-way ANOVA test will determine sex and population variation. Age within a population will be analysed with a within-group regression. Validation tests will be performed to determine the accuracy of the newly discovered prediction protocols developed and identified from the research. This might involve conducting a series of “blind” facial approximations, where antemortem images are available for comparison post completion.

Dialogical Fingerprinting

Godfrey Inyama[1], Jacky Visser[2], Chris Reed[3]

[1] Centre for Argument Technology, University of Dundee, 2564837@dundee.ac.uk

[2] jvisser@dundee.ac.uk

[3] c.a.reed@dundee.ac.uk

Abstract

The prevalence of discourse in the digital spaces between known and unknown individuals or groups has resulted in a trend where individuals withhold expressing their opinions due to fear of identification, tracking, and potential repercussions. Certain research thus far has proven that individuals engage in discourse in unique ways. The concept of extracting and affirming this uniqueness is known as "Dialogical Fingerprinting" (Foulis et al., 2020). My research aims to potentially use various cutting edge machine learning techniques to discover, analyse, and evaluate these dialogical fingerprints. In this abstract, the terms argument, discourse, and dialogue are used interchangeably with same meanings.

To fully understand this uniqueness in dialogue patterns, I will be training large language models such as Bidirectional Encoder Representations from Transformers (BERT), Transformer-XL, and Generative Pre-trained Transformer 3 (GPT-3) over large dialogue datasets which have been gathered from multiple sources. The primary datasets I will be training the models with have been manually annotated and stored in a semi-structured layout using JSON language. This type of datasets also follows the pattern of the Argument Interchange Format (AIF), which is a formal representational way for arguments (Chesñevar et al., 2006). These types of datasets are currently stored in the Argument Interchange Format Database (AIFdb) which is the most comprehensive argument corpora presently, and it is publicly accessible.

From the Datasets, the main dialogical fingerprint which would be found is the intent in dialogues. This process is called illocutionary parsing (Budzynska et al., 2016). From the Datasets, the intents behind dialogues are found in the argument structure. To extract these, the machine learning models listed above would be trained over the train sets, tested over the test sets, and finally evaluated to get their performances.

Other Datasets would be annotated before being used. Research is currently ongoing on how to automate the annotation process of argument datasets. This process is known as argument mining (Lawrence & Reed, 2019).

Two notabilities about my research are, developing a base infrastructure which would connect the argument mining methods with the dialogical fingerprint extraction models, and also testing and evaluating the stability of these models over multilingual annotated datasets.

References

Budzynska, K., Janier, M., Reed, C., & Saint-Dizier, P. (2016). Theoretical foundations for illocutionary structure parsing. *Argument & Computation*, *7*(1), 91-108.

Chesnevar, C., Modgil, S., Rahwan, I., Reed, C., Simari, G., South, M., ... & Willmott, S. (2006). Towards an argument interchange format. *The knowledge engineering review*, *21*(4), 293-316.

Foulis, M., Visser, J., & Reed, C. (2020). Dialogical Fingerprinting of Debaters. Computational Models of Argument, 465–466. https://doi.org/10.3233/FAIA200536.

Lawrence, J., & Reed, C. (2020). Argument mining: A survey. *Computational Linguistics*, *45*(4), 765-818.

University of Dundee

How machine learning algorithms can analyse argument mining

Somaye Moslemnejad[1], Chris Reed[2], John Lawrence[3]

[1] University of Dundee, 2538466@dundee.ac.uk

[2] c.a.reed@dundee.ac.uk

[3] j.lawrence@dundee.ac.uk

Abstract

Argumentation mining has been defined as the automated detection of the argumentation structure and classification of both its component elements and their argumentative relationships (John Lawrence et al., 2019). When sufficient explicit discourse markers are present in utterances, argumentation can be interpreted by the machine with an acceptable degree of accuracy (Marie-Francine et al., 2018). However, the mining task is difficult due to the lack or ambiguity of the discourse markers, and the fact that a substantial amount of knowledge needed for the correct recognition of the argumentation, its composing elements and their relationships is not explicitly present in the text, but makes up the background knowledge that humans possess when interpreting language (Alexandros Vassiliades et al., 2021). In the research, we focus on how the machine can automatically acquire the needed common sense and world knowledge. The main goal of the research is applying machine learning (ML) algorithms to argument mining (AM), which aims to automatically extract arguments from generic textual corpora and structured data in order to acquire needed common sense for computational models.

Some tasks have been done so far in the previous works to mine automatically argumentation using ML including relation or link prediction between arguments (Marco Lippi et al., 2016). We have also worked on this using support vector machine (SVM) to classify attack and support relations between arguments in a large data set, namely the 2016 US presidential elections, which includes annotations of selected excerpts of primary and general election debates, combined with annotations of selected excerpts of corresponding Reddit megathreads, and the inter-textual correspondence between the televised debates and the Reddit comments, from the AIFdb repository. A small section of the used data set is shown in Figure 1 which indicates information and locutions nodes between speakers in the data set and their relations. In addition, connected locutions of speakers in the mentioned data set have been classified using same ML classifier, say SVM, with python language programming, and some evaluations metrics are measured like F1 score which 50% has been achieved. Also, some baseline methods have been considered for same project such as BERT as a transformer model and Gloove text embedding which 49% and 51% accuracy have been achieved respectively. After that, we aim to find an algorithm to improve accuracy and pursue knowledge resources beyond the relations in argumentation, and we would like to migrate to deep learning as a strong ML model to extract knowledge accurately.

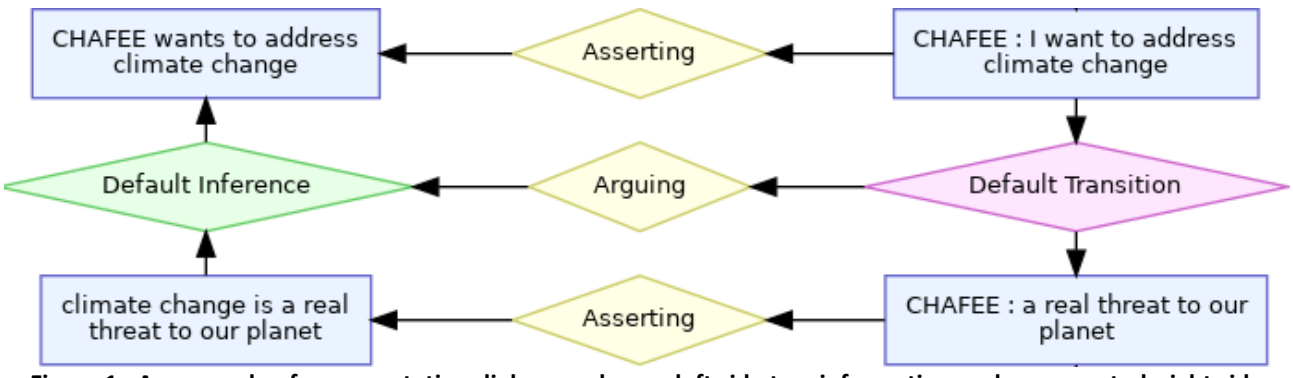

Figure 1: An example of argumentation dialouge scheme; left side two information nodes connceted; right side speakers locutions connected; middle side connection between information nodes and locution nodes

References

Marie-Francine Moens,(2018). Argumentation mining: How can a machine acquire common sense and world knowledge?. *Argument & Computation,* 9: 1-14.

Marco Lippi, Paolo Torroni,(2016). Argument Mining: A Machine Learning Perspective. *International Workshop on Theory and Applications of Formal Argumentation, 163–176*.

John Lawrence, Chris Reed, (2019). Argument Mining: A Survey. Computational Linguistics 45 (4): 765–818.

Alexandros Vassiliades, Nick Bassiliades, Theodore Patkos, (2021). Argumentation and explainable artificial intelligence: a survey. Cambridge University Press,

Tools for Managing Argumentative Dialogue

Nicole Orr[1], John Lawrence[2], Chris Reed

[1] University of Dundee, 170010591@dundee.ac.uk

[2] j.lawrence@dundee.ac.uk

[3] c.a.reed@dundee.ac.uk

Abstract

My research is focusing on exploring solutions for managing argumentative dialogue. This involves the creation of a database and an agent API to process and execute any dialogue games which are specified through the Dialogue Game Description Language, DGDL (Wells & Reed, 2012). This is a domain specific language that is used to describe dialectical games. The software builds upon the Dialogue Game Execution Platform, DGEP (Bex et al., 2014), which manages a structured dialogue according to a protocol specified through DGDL for human and virtual participants. DGEP uses a centralised system to manage each instance of a dialogue game for its participants. The software instead uses distributed systems to allow each agent to manage itself according to its own specified protocol. This enables agents running different dialogue games to engage with each other within the one dialogue. The separate components used are shown in Figure 1.

The agent API consists of two components, a backend to process the dialogue and a frontend to control the agent and enable both autonomous agents and human interfaces to take part in dialogues. The frontend receives a pointer to a DGDL file which the backend processes and then manages the agent according to. The backend also maintains the agent's own commitment store throughout the dialogue. Each individual agent sends and receives updates to the dialogue to and from the dialogue as a service database, DaaSdb, using an extended version, xAIF, of the language of the Argument Interchange Format, AIF, ontology (Chesñevar et al. 2006). Using AIF ensures the software's compatibility with AIFdb (Lawrence et al. 2012), the Argument Web and the wider Semantic Web. The software stores and manages the extra dialogue information within the DaaSdb before sending the AIF representation of the dialogue to AIFdb. AIFdb is used to store and manage the dialogues' histories which captures the order history of locutions uttered and the underlying argument structures within the dialogue. Each time an agent engages in the dialogue game it will send xAIF representing its interaction that will be added to the dialogue history by AIFdb. AIFdb and the Argument Web can also be used as a large knowledge base within the dialogue games for realistic multi-agent dialogues. The main challenge going forward with my research is managing multi-agent dialogues where each agent is using a very different DGDL protocol and handling agents breaking the rules of their specified dialogue games.

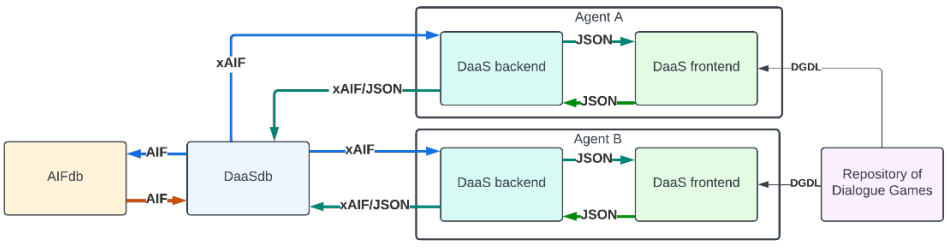

Figure 1: Software components for managing argumentative dialogue

References

F. Bex, J. Lawrence, C. Reed (2014). Generalising argument dialogue with the Dialogue Game Execution Platform. In: S. Parsons, N. Oren, C. Reed, F. Cerutti, editors. *Fifth International Conference on Computational Models of Argument* (COMMA 2014). IOS Press p. 141–152.

C. Chesñevar, J. McGinnis, S. Modgil, I. Rahwan, C. Reed, G. Simari, M. South, G. Vreeswijk, and S. Willmott (2006). Towards an argument interchange format. *The Knowledge Engineering Review*, 21(4): 293–316.

J. Lawrence, F. Bex, C. Reed, M. Snaith (2012). AIFdb: infrastructure for the argument web. In: Verheij B, Szeider S, Woltran S, editors. *Fourth International Conference on Computational Models of Argument* (COMMA 2012). IOS Press p. 515–516.

S. Wells and C. Reed (2012). A domain specific language for describing diverse systems of dialogue. *Journal of Applied Logic*, 10(4):309–329.

Exploring the use of AAC to facilitate the communication of children and young people with Down syndrome.

Elaine Scougal[1], Professor Annalu Waller[2], Professor Alissa Melinger[3]

[1] School of Science and Engineering, e.scougal@dundee.ac.uk
[2] a.waller@dundee.ac.uk
[3] Division of Psychology, a.melinger@dundee.ac.uk

Abstract

Communication provides the foundation of relationships. Due to factors such as verbal dysfluency and low intelligibility, many people with Down syndrome experience verbal communication impairments throughout life, potentially impacting relationships with others and participation in society. Early intervention is, therefore, important in enabling individuals with Down syndrome to reach their potential in terms of communication and independence. Augmentative and Alternative Communication (AAC) can enable the exchange of thoughts and stories in the absence of, or in addition to, speech, including the use of signing, symbols, and electronic communication aids that enable digital voice output (See Figure 1). Despite the prevalence of speech challenges within this group and the value of early intervention, research into the use of AAC to support the communication of children and young people with Down syndrome is limited. The aims of this project are 1) to explore how children and young people with Down syndrome and stakeholders perceive and use AAC to support communication with familiar and new communication partners, 2) to explore experiences of support related to communication and AAC, and 3) to provide insights into how children and young people with Down syndrome with limited verbal communication can best be supported to engage meaningfully in research activities.

The project utilises a mixed-methods approach, beginning with the development and online distribution of a survey, completed by primary caregivers of children and young people with Down syndrome (aged 3 to 18 years; n=264). The survey gathered both quantitative and qualitative data, providing insights relating to their child's communication methods and abilities in addition to their own perceptions and experiences relating to AAC. Analysis of the data highlighted keyword signing as the most common form of AAC used by this group. Electronic AAC, in contrast, was used by less than 6% of the sample. Barriers relating to support, context, and communication partner skill emerged from the data, motivating in-depth exploration of experiences of those using AAC, particularly added AAC such as communication books and devices, via a series of case studies within the next phase of the research. Employing qualitative data collection and analysis techniques, insights will be gained from children and young people with Down syndrome and stakeholders (e.g., caregivers, siblings, speech therapists, and educators). Data will be triangulated from an array of methods, including semi-structured interviews and Talking Mats™ (a visual discussion tool) in addition to diary- and photography-based tasks. Combined, this project will provide scope for enhancing the communication, agency, and independence of people with Down syndrome across the lifespan.

Figure 1: A child with Down syndrome using a voice output communication aid

University of Dundee

Multi-Modal Alignment for Radiology Report Generation Based on Conditional Reports

Chenyu Wang[1], Stephen McKenna[2], Vladimir Janjic[3]

[1] University of Dundee, 2410984@dundee.ac.uk

[2] s.j.z.mckenna@dundee.ac.uk

[3] vjanjic001@dundee.ac.uk

Abstract

With the development of medical imaging technology, X-ray images have become an essential tool for the analysis and treatment of various diseases. However, reading and interpreting medical images require highly skilled medical professionals with extensive experience, leading to an enormous burden on medical resources and doctors. Therefore, the automatic generation of radiology reports has become a crucial research area in recent years. Existing research [1][2][3] in this area has made significant progress, but there are still some spaces for improving the accuracy of generated reports.

I proposed a multi-modal alignment method (as shown in Figure 1) based on retrieved similar reports for radiology report generation. Given a medical image, the method employs five steps to generate a report: 1) to share the majority of the content, we first retrieve a related medical report (conditional report) from a similar patients in the training dataset; 2) then apply an image encoder (e.g. a standard CNN) for image representation learning and a text encoder for text representation; 3) then concatenating the image representation and text representation and apply a self-attentional transformer to self-discover their region-to-region relationships; 4) then apply a extractor to extract the composite features from the concatenated representation; 5) finally the composite features are fed to a standard Transformer [4] and try to be aligned with the target text.

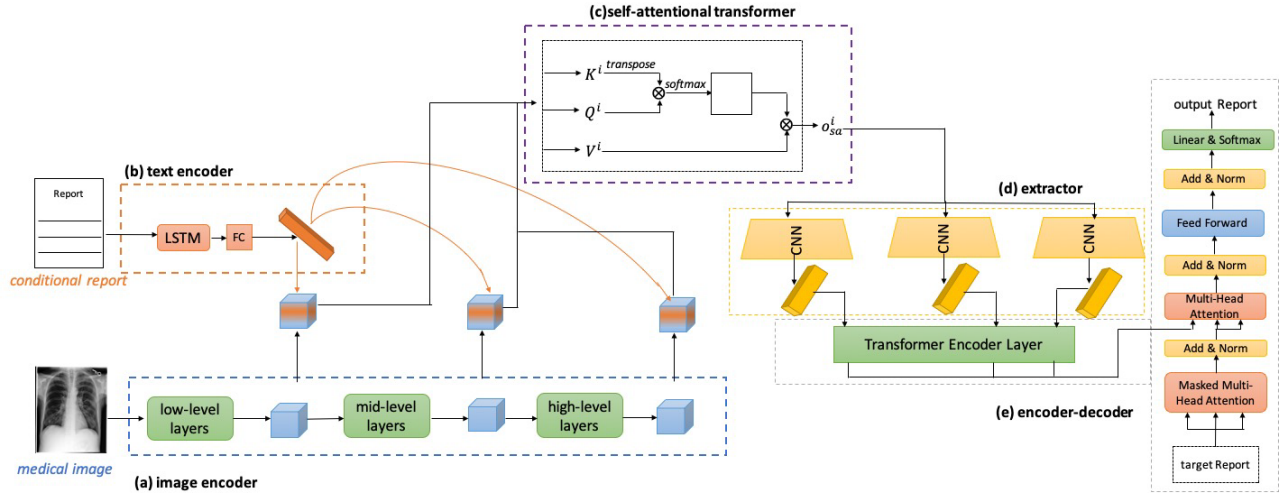

Figure 1: The overall architecture of my proposed method. Given an input medical image, our goal is to generate a medical report corresponding to the input medical image. It contains five main components: (a) image encoder, (b) text encoder, (c) self-attentional transformer, (d) composite feature extractor and (e) a standard Transformer

References

Qin, H. and Song, Y., 2022, May. Reinforced cross-modal alignment for radiology report generation. In Findings of the Association for Computational Linguistics: ACL 2022 (pp. 448-458).

Song, X., Zhang, X., Ji, J., Liu, Y., & Wei, P. (2022, October). Cross-modal Contrastive Attention Model for Medical Report Generation. In Proceedings of the 29th International Conference on Computational Linguistics (pp. 2388-2397).

Chen, Z., Song, Y., Chang, T. H., & Wan, X. (2020). In Proceedings of the 2020 Conference on Empirical Methods in Natural Language Processing (EMNLP), pages 1439–1449, Online.

Vaswani, A., Shazeer, N., Parmar, N., Uszkoreit, J., Jones, L., Gomez, A. N., ... & Polosukhin, I. (2017). Attention is all you need. Advances in neural information processing systems, 30.

University of Dundee

Comparison of a newly developed fluorescent nanobiosensor to ion mobility spectrometry for the detection of cocaine

Kathryn Burton[1], Lorna Nisbet[2], Niamh Nic Daeid[3], Oluwasesan Adegoke[4]

[1] Leverhulme Research Centre for Forensic Science, 2431431@dundee.ac.uk

[2] lnisbet001@dundee.ac.uk

[3] n.nicdaeid@dundee.ac.uk

[4] o.adegoke@dundee.ac.uk

Abstract

In 2021, 30% of all drug misuse deaths in Scotland involved cocaine (National Records of Scotland, 2022). The European Monitoring Centre for Drugs and Drug Addiction (EMCDDA) estimates that in 2021 approximately 3.5 million people in Europe aged 15-64 took cocaine at least once within that year, with lifetime prevalence being 14.4 million (EMCDDA, 2022). In 2020, 1982 tons of pure cocaine was estimated to have been produced, an increase of 11% on 2019, and more than double 2014 figures; with 1424 tons of cocaine of varying purity being seized globally, an increase of 4.5% on 2019 (UNODC, 2022).

Quick and accurate identification of seized substances by forensic drug chemists (and trained field personnel) is important for healthcare and judicial systems. Ion mobility spectrometry (IMS) is an established analytical technique used in prisons and at border security to rapidly check for explosive materials and illicit drugs (Norman et al., 2021). Potential for overlapping signals along with difficulty in analysing complex mixtures can lead to false negatives and false positives. IMS equipment can be easily overloaded so the amount of substance sampled must be accurately measured, which can be difficult in field situations (Denia et al., 2022). A relatively recent area of interest in terms of substance identification is the use of nanobiosensors. Proof-of-concept publications introduce the idea of nanobiosensors for forensic detection. Previously published literature – such as Adegoke et al., 2020, 2019; Burton et al., 2022; Chen et al., 2008; Mao et al., 2017; Zhang and Johnson, 2009; and Zhang et al., 2016 – indicate their high selectivity. However, the range of compounds tested is often very limited, and so further testing is required.

This research compares a newly developed fluorescent nanobiosensor for the detection of cocaine with the established IMS technique produced by Rapiscan ®, by testing the limit of detection (LoD) of cocaine and testing the selectivity of cocaine against other compounds including controlled drugs and cutting agents commonly encountered in cocaine street samples, of both techniques.

The newly developed amphiphilic polymer (A-polym)-functionalised ZnSe/In_2S_3 core/shell quantum dots (QDs) electrostatically linked to cationic cetyltrimethylammonium bromide (CTAB)-capped gold nanoparticles (AuNP) and conjugated with an MNS 4.1 anticocaine thiolated DNA aptamer (Aptm) formed a fluorescent nanoprobe (Aptm-A-polym-QDs-AuNP) which is sensitive to cocaine, with a LoD of 242.7 ng, though not as low as the Rapiscan ® 3E IMS's LoD of 20 ng. Both the nanobiosensor and IMS system resulted in some false positive results with IMS showing cross-reactivity with the opiates mixture, and the nanobiosensor showing cross-reactivity with nicotine, phenacetin and the drug mixtures. Further testing will be undertaken by examining each component of the mixtures separately to identify which are cross-reactive for each detection technique.

References

Adegoke, O., McKenzie, C., NicDaeid, N., 2019. Multi-shaped cationic gold nanoparticle-l-cysteine-ZnSeS quantum dots hybrid nanozyme as an intrinsic peroxidase mimic for the rapid colorimetric detection of cocaine. Sens. Actuators B Chem. 287, 416–427. https://doi.org/10.1016/j.snb.2019.02.074

Adegoke, O., Pereira-Barros, M.A., Zolotovskaya, S., Abdolvand, A., NicDaeid, N., 2020. Aptamer-based cocaine assay using a nanohybrid composed of ZnS/Ag2Se quantum dots, graphene oxide and gold nanoparticles as a fluorescent probe. Microchim. Acta 187, 104. https://doi.org/10.1007/s00604-019-4101-6

Burton, K., Nic Daeid, N., Adegoke, O., 2022. Surface plasmon-enhanced aptamer-based fluorescence detection of cocaine using hybrid nanostructure of cadmium-free ZnSe/In2S3 core/shell quantum dots and gold nanoparticles. J. Photochem. Photobiol. Chem. 433, 114131. https://doi.org/10.1016/j.jphotochem.2022.114131

Chen, J., Jiang, J., Gao, X., Liu, G., Shen, G., Yu, R., 2008. A New Aptameric Biosensor for Cocaine Based on Surface-Enhanced Raman Scattering Spectroscopy. Chem. - Eur. J. 14, 8374–8382. https://doi.org/10.1002/chem.200701307

Denia, A., Esteve-Turrillas, F.A., Armenta, S., 2022. Analysis of drugs including illicit and new psychoactive substances in oral fluids by gas chromatography-drift tube ion mobility spectrometry. Talanta 238, 122966. https://doi.org/10.1016/j.talanta.2021.122966

EMCDDA, 2022. European drug report: trends and developments.

Mao, K., Yang, Z., Li, J., Zhou, X., Li, X., Hu, J., 2017. A novel colorimetric biosensor based on non-aggregated Au@Ag core–shell nanoparticles for methamphetamine and cocaine detection. Talanta 175, 338–346. https://doi.org/10.1016/j.talanta.2017.07.011

National Records of Scotland, 2022. Drug-related deaths in Scotland in 2021.

Norman, C., McKirdy, B., Walker, G., Dugard, P., NicDaéid, N., McKenzie, C., 2021. Large-scale evaluation of ion mobility spectrometry for the rapid detection of synthetic cannabinoid receptor agonists in infused papers in prisons. Drug Test. Anal. 13, 644–663. https://doi.org/10.1002/dta.2945

UNODC, 2022. 4 World Drug Report 2022. UNITED NATIONS, S.l.

Zhang, C., Johnson, L.W., 2009. Single Quantum-Dot-Based Aptameric Nanosensor for Cocaine. Anal. Chem. 81, 3051–3055. https://doi.org/10.1021/ac802737b

Zhang, Y., Sun, Z., Tang, L., Zhang, H., Zhang, G.-J., 2016. Aptamer based fluorescent cocaine assay based on the use of graphene oxide and exonuclease III-assisted signal amplification. Microchim. Acta 183, 2791–2797. https://doi.org/10.1007/s00604-016-1923-3

Balancing The Scales of Justice: The Communication of Scientific Evidence and the Impact on Case Progression and Prosecution Decision-Making in Scotland since 2009

Simon-Lewis Menzies[1], Prof Lucina Hackman[2], Dr Herve Menard[3]

[1] Leverhulme Research Centre for Forensic Science, University of Dundee, 080007503@dundee.ac.uk

[2] l.hackman@dundee.ac.uk

[3], h.menard@dundee.ac.uk

Abstract

The criminal justice system can often be likened to a machine with intricate interactions between constituent cogs. Some such cogs in the machine are scientific evidence, its communication, and how it affects the decision-making process in respect of case progression. Though there is a wider machine of criminal justice, there are sometime disparities in how different types of cases progress through the criminal justice system. Sexual and non-sexual violent crimes can be some of the most difficult to progress through the criminal justice system. Since 2009, there have been several legislative changes aimed at tackling case attrition. The overarching aim of this thesis was to understand the role of the communication of scientific evidence and to what extent it impacts case progression and prosecution decision-making in serious sexual and non-sexual violent crime in Scotland since 2009 This thesis examines the issues of case progression, investigation, and prosecution through a novel approach by conducting research in three data collection phases and objectives. The first being to examine the communication of scientific evidence and decision-making involved during the investigation and prosecution of rape cases in Scotland from an organisation that is independent of the criminal justice process, Rape Crisis Scotland, to gain insight into the handling of rape cases in Scotland from an alternative viewpoint. Findings suggest real discrepancies in how national criminal justice agencies operate showing that although there may be a national framework, this is not always the reality in different regions of Scotland. The second objective was to determine to what extent, if any, variations in methods of communication of uncertainty affects decision-making in criminal justice case progression – specifically the decision to prosecute a case and the confidence in that decision. Data collected this citizen science project which shows there are small intricacies in how different groups decide whether to prosecute cases and the confidence in which they make those decisions. The final objective was to determine to what extent potential jurors attribute trust and weight to different evidence types when presented with them in a criminal case. The potential juror pool in Scotland being largely made up of non-scientifically trained lay people. This final phase showed that there are subtle differences in how different groups attribute trust and weight as potential jurors in different criminal cases based on their engagement with popular culture representations of crime and criminal justice. These phases combine to illustrate the processes involved in sexual and non-sexual violent crime case progression in Scotland since 2009 in a new way to show that many of the criminal justice reforms in Scotland have had little or no impact on case progression. Moreover, there is limited evidence to suggest that there are subtle differences between how those who have previously served as a juror compared with those that have not, interact with different types of evidence in different type of crimes as well as their decisions and decision confidence in prosecutions. Key recommendations for policy and future research are made and discussed.

Stability Analysis for Laminar Flows for Asymmetric Case

Shen Hong[1], Ping Lin[2]

[1] School of Science and Engineering, shong@dundee.ac.uk

[2] p.lin@dundee.ac.uk

Abstract

The research will extend the recent analysis of Multiple solutions and their asymptotic for laminar flows through a porous channel with different permeabilities of symmetric cases and asymmetric cases. This report will mainly analyse the stability of three solutions for the laminar fluid flow through a porous channel with different permeabilities, which is an asymmetric case. Eigenvalue problems associated with stability problems for the constructed fluid flow will be formulated and solved by a finite difference method numerically for temporal stability analysis.

Laminar flows have been broadly studied during the decades. The normal structure of the suction or injection flows was firstly built with Navier-Stokes equations (Berman et al., 1953). During the decades, the study used dimensionless equations to analyze the problem and asymptotic solutions of three types were found for the both symmetric case and asymmetric case. The laminar flow happens at the lower speed and the speed is decided by the Reynolds number. As we reexamine the recent work of Multiple asymptotic solutions for laminar flows for the asymmetric case (Figure 1), it suggested that there are three types of solutions as type *I*, type *II*, and type *III* for the asymmetric case (Guo et al., 2020). Three types were solved numerically with boundary conditions on $y = 1$ and $y = -1$. The types *I* and *II* are different by different exponentially small terms for the large suction Reynolds number, while type *III* solution was shown with a complicated structure. We analysed the Navier-Stokes equations by investigating the linear stability based on dimensionless equations. Equations for solving eigenvalues $s(Re(s))$ are shown as below.

$$\begin{cases} \hat{u}_x + \hat{v}_y = 0, \\ (F_y\hat{u} + xF_{yy}\hat{v}) + (xF_y\hat{u}_x - F\hat{u}_y) - \frac{1}{Re}(\hat{u}_{xx} + \hat{u}_{yy}) + \hat{p}_x = -s\hat{u}, \\ (-F_y\hat{v}) + (xF_y\hat{v}_x - F\hat{v}_y) - \frac{1}{Re}(\hat{v}_{xx} + \hat{v}_{yy}) + \hat{p}_y = -s\hat{v}. \end{cases}$$

The real part of $s(Re(s))$ shows the growth or decay of the perturbation. And it represents the stability of functions. The staged grid method was used to deal with lack of the boundary conditions of pressure and also the finite difference scheme was also used for solving equations. We investigated that there are negative and positive numbers for the real part of the eigenvalues of all the three types of solutions. Hence, we found out that the three types of solutions are unstable.

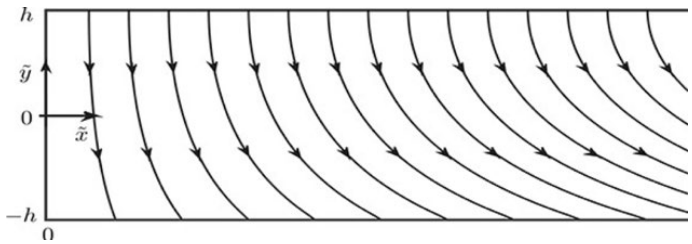

Figure 1: Asymmetric fluid pattern

References

A.S. Berman (1953). Laminar flow in channels with porous walls. *Applied Physics*, 24(9):1232–5.

H. Guo, C. Gui, P. Lin (2020). Multiple solutions and their asymptotics for laminar flows through a porous channel with different permeabilities. *IMA Journal of Applied Mathematics*, 85:280–308.

Experimental study of sequential high density turbidity currents and their deposits in response to a simultaneous slope break and loss of confinement

Jonathan Wilkin[1], Alan Cuthbertson[2], Sue Dawson[3], Dorrik Stow[4], Karl Stephen[5], Uisdean Nicholson[6]

[1] Civil Engineering, University of Dundee, jzwilkin@dundee.ac.uk

[2] ajscuthbertson@dundee.ac.uk

[3] Division of Energy, Environment and Society; UNESCO Centre for Water Law, Policy and Science, University of Dundee, s.dawson@dundee.ac.uk

[4] Institute of GeoEnergy Engineering, Heriot-Watt University, dorrik.stow@pet.hw.ac.uk

[5] k.d.stephen@hw.ac.uk

[6] u.nicholson@hw.ac.uk

Abstract

Results are presented from a series of scaled laboratory experiments to explore how sequential high-density turbidity currents (HDTCs) with different volume fluxes (Q_0 = 10.2 - 13.5 m^3/hr) and initial volumetric sediment concentrations (c_0 = 0.12 - 0.16) respond to different slope break (SB) angles (5° - 9°) at a simultaneous loss of confinement (LOC). The study investigates the impact of the SB-LOC on the stacking pattern of the basin deposits produced by the sequential HDTCs. Of particular interest is the effect that antecedent HDTCs and their deposits have on the subsequent HDTC dynamics and how this feedback drives the evolution of basin depositional features. Each experimental run consists of three or four sequential HDTCs that are scaled on non-dimensional parameters for the flow properties (i.e. densimetric Froude and Reynolds numbers) and sedimentary conditions (i.e. Shields and Rouse numbers) (e.g. de Leeuw et al., 2016). Results indicate that on reaching the SB-LOC, the peak flow velocities within the HDTCs range between 0.88 m/s and 1.29 m/s. Immediately downstream of the SB-LOC the HDTCs collapse towards the bed and expand radially into the basin (i.e. flow relaxation,), resulting in higher shear velocities. This transition from two- and three-dimensional flow processes causes the HDTCs to produce a channel-lobe transition zone (CLTZ) immediately downstream of the SB-LOC.

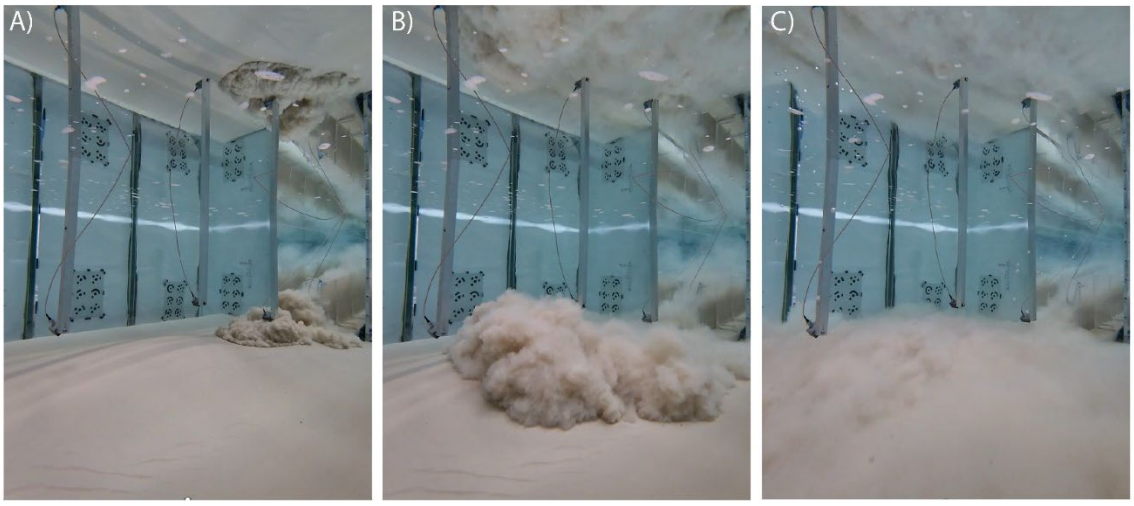

Figure 1: The expansion of a HDTC (Series 2, Run 03, c_0 = 12%, α =7°) downstream of the SB-LOC at; (A) 1.5 seconds, (B) 3.5 seconds, and (C) 10 seconds. Note in B how the head of the HDTC appears to bifurcate around the crest of the antecedent lobe topography.

Although these CLTZs are maintained over subsequent HDTCs, they typically shorten as the centroids of the individual lobe deposits occur within increasing proximity to the feeder channel and SB-LOC. Ultrasonic velocity profile measurements demonstrate that the depositional topography reduces the centerline velocity of sequential HDTCs, whilst deposit maps highlight how sedimentation is topographically steered towards the flanks (Fig. 1B) of the evolving lobe deposit. Results therefore highlight the mechanisms that drive lobe deposition downstream of a SB-LOC and provide an insight into how HDTCs form and maintain CLTZs. To build upon these observations a sedimentological field study was undertaken in the Tabernas Basin, SE Spain, funded in part by the 2020 David Smith Award. The aim of which was to better understand the sedimentological products of supercritical high-density turbidity currents, with a particular focus on deposits formed in an area believed to be analogous to the SB-LOC of the laboratory experiments.

References

De Leeuw, J., Eggenhuisen, J.T. and Cartigny, M.J.B. (2016) Morphodynamics of submarine channel inception revealed by new experimental approach. Nat. Commun.,7,1–7.